Cellular and Molecular Life Sciences (2024) 81:336
https://doi.org/10.1007/s00018-024-05385-y

ORIGINAL ARTICLE

Overexpression of long noncoding RNA DUXAP8 inhibits ER-phagy through activating AKT/mTOR signaling and contributes to preeclampsia

Xiao-Hong Wei[1] · Ling-Yun Liao[1] · Yang-Xue Yin[1] · Qin Xu[1] · Shuang-Shuang Xie[1] · Min Liu[1] · Lin-Bo Gao[2] · Hong-Qin Chen[1] · Rong Zhou[1]

Received: 5 April 2024 / Revised: 9 July 2024 / Accepted: 29 July 2024

Abstract

Preeclampsia (PE) is a life-threatening pregnancy-specific complication with controversial mechanisms and no effective treatment except delivery is available. Currently, increasing researchers suggested that PE shares pathophysiologic features with protein misfolding/aggregation disorders, such as Alzheimer disease (AD). Evidences have proposed defective autophagy as a potential source of protein aggregation in PE. Endoplasmic reticulum-selective autophagy (ER-phagy) plays a critical role in clearing misfolded proteins and maintaining ER homeostasis. However, its roles in the molecular pathology of PE remain unclear. We found that lncRNA DUXAP8 was upregulated in preeclamptic placentae and significantly correlated with clinical indicators. DUXAP8 specifically binds to PCBP2 and inhibits its ubiquitination-mediated degradation, and decreased levels of PCBP2 reversed the activation effect of DUXAP8 overexpression on AKT/mTOR signaling pathway. Function experiments showed that DUXAP8 overexpression inhibited trophoblastic proliferation, migration, and invasion of HTR-8/SVneo and JAR cells. Moreover, pathological accumulation of swollen and lytic ER (endoplasmic reticulum) was observed in DUXAP8-overexpressed HTR8/SVneo cells and PE placental villus trophoblast cells, which suggesting that ER clearance ability is impaired. Further studies found that DUXAP8 overexpression impaired ER-phagy and caused protein aggregation medicated by reduced FAM134B and LC3II expression (key proteins involved in ER-phagy) via activating AKT/mTOR signaling pathway. The increased level of FAM134B significantly reversed the inhibitory effect of DUXAP8 overexpression on the proliferation, migration, and invasion of trophoblasts. In vivo, DUXAP8 overexpression through tail vein injection of adenovirus induced PE-like phenotypes in pregnant rats accompanied with activated AKT/mTOR signaling, decreased expression of FAM134B and LC3-II proteins and increased protein aggregation in placental tissues. Our study reveals the important role of lncRNA DUXAP8 in regulating trophoblast biological behaviors through FAM134B-mediated ER-phagy, providing a new theoretical basis for understanding the pathogenesis of PE.

Keywords Preeclampsia · DUXAP8 · ER-phagy · FAM134B · Trophoblast cells

Xiao-Hong Wei and Ling-Yun Liao contributed equally to this work.

✉ Rong Zhou
zhourong_hx@scu.edu.cn

[1] Department of Obstetrics and Gynecology, Key Laboratory of Birth Defects and Related Diseases of Women and Children (Sichuan University) , Ministry of Education, West China Second University Hospital, Sichuan University, NHC Key Laboratory of Chronobiology, Sichuan University, Chengdu, Sichuan, P.R. China

[2] Center for Translational Medicine, Key Laboratory of Birth Defects and Related Diseases of Women and Children (Sichuan University), Ministry of Education, Department of Obstetrics and Gynecology, West China Second University Hospital, Sichuan University, Chengdu, Sichuan 610041, P.R. China

Published online: 09 August 2024

Abbreviations

PE	Preeclampsia
lncRNA	Long noncoding RNA
ER-phagy	Endoplasmic reticulum-selective autophagy
ASO	Antisense Oligonucleotide
LIR	LC3-binding region
Ad	Adenovirus
GD	Gestational day
sFlt-1	Soluble fms-like tyrosine kinase 1

Introduction

Preeclampsia (PE) is a life-threatening pregnancy-specific complication characterized by hypertension after 20 weeks of gestation and accompanied by multiple organ system involvement. It is a major cause of increased maternal and fetal morbidity and mortality, affecting approximately 5–7% of pregnant women worldwide [1, 2] and causing approximately 70,000 maternal and 500,000 perinatal deaths per year [3, 4]. Despite substantial research and improvement, the pathophysiological mechanisms of PE still remain controversial and no effective treatment except delivery is available. Therefore, elucidation of the specific pathogenesis of PE has been considered the chief challenge to be solved urgently.

PE is considered a placenta-derived disease owing to the rapid remission of its clinical manifestations in patients after pregnancy termination [5–7].Insufficient trophoblast infiltration and spiral artery remodeling disorders at the maternal-fetal interface are believed to be the pathological bases of PE [1, 2].In more recent years, a growing number of researchers suggested that PE shares pathophysiologic features with protein misfolding/aggregation disorders, such as Alzheimer disease(AD) [8–10]. The accumulation of cytotoxic aggregated proteins in urine, serum and placentas of PE patients has been detected and protein aggregation in trophoblasts is associated with insufficient trophoblast invasion and dysfunctional uterine spiral artery remodeling [10–13]. Thus, further exploration of the mechanisms underlying protein aggregation in placenta is crucial to improve our understanding of PE pathophysiology.

(Macro)autophagy is a process of non-selective degradation to maintain cellular homeostasis through which cells clear damaged macromolecules such as aggregated proteins, and intracellular components like organelles [14]. Several studies have proposed defective autophagy as a potential source of protein aggregation in PE [15–17].Evidence showed that autophagy-deficient trophoblasts exhibited poor invasion and worse ability to induce vascular remodeling [8, 18, 19]. In addition to nonselective degradation of autophagosomes, autophagy also acts selectively on specific organelles or cellular components through a "cargo-ligand-receptor" mode to maintain cellular homeostasis [20].

The endoplasmic reticulum (ER) is the primary site for protein synthesis, folding, and modification [21]. Endoplasmic reticulum-selective autophagy (ER-phagy) is a type of organelle autophagy characterized by the specificity of the autophagosome membrane wrapping the membrane structure of the double-layered ER [22]. It plays a critical role in clearing misfolded proteins and maintaining ER homeostasis [23]. FAM134B, also known as JK-1 or RETREG1 (reticulophagy regulatory factor 1), is the first ER-phagy receptor found in mammalian cells [22]. An LIR (LC3 interaction region) in the C-terminus of the FAM134B protein binds to LC3/GABARAP protein and targets ER fragments into autophagic vesicles [24]. The impairment of ER-phagy results in aggregation of misfolded proteins and abnormal ER. Recently, studies have found that ER-phagy disorders can lead to a variety of neurodegenerative diseases [25]. For example, FAM134B-mediated impaired ER-phagy is associated with Niemann-Pick Type C Disease, a fatal progressive neurodegenerative disease [26].

Long noncoding RNAs (lncRNAs) are a class of noncoding RNAs greater than 200 nucleotides in length. They have multiple functions and participate in various biological processes, such as transcription, post-transcriptional regulation, and epigenetic modification [27]. An increasing number of studies have shown that lncRNAs are involved in regulating the biological behavior of placental trophoblasts through multiple mechanisms and signaling pathways. The role of lncRNA DUXAP8 in regulating the biological behavior of tumor cells and the occurrence and development of various tumors, including non-small cell lung [28], bladder [29], and ovarian [30] cancer, has also been documented. For example, DUXAP8 activates the Akt/mTOR signaling pathway and promotes tumor occurrence, and DUXAP8 overexpression can promote radiation resistance in breast cancer cells by regulating the PI3K/AKT/mTOR pathway and the EZH2-E-cadherin /RHOB axis [31]. However, whether lncRNA DUXAP8 regulates the biological behavior of trophoblast cells through ER-phagy has not been reported.

Here, we demonstrated that lncRNA DUXAP8 level was upregulated in the placentae of PE patients and significantly correlated with clinical indicators. Functional experiments showed that the upregulation of DUXAP8 inhibited the proliferation, migration, and invasion of HTR8/SVneo and JAR cells. Furthermore, we firstly provided evidence in vivo and in vitro that DUXAP8 plays an important role in the pathogenesis of PE by modulating FAM134B-mediated ER-phagy through AKT/mTOR signaling. This study provides a new theoretical basis for exploring the potential biomarkers and prevention targets of PE.

Materials and methods

Sample collection

The collection and treatment of human placenta tissues were done in accordance with the ethical principles of the Declaration of Helsinki and approved by the Ethics Committee of West China Second Hospital of Sichuan University (Medical Research-2019-032) [1]. All participants provided informed consent. A total of 86 subjects were enrolled from the West China Second Hospital of Sichuan University, including 46 normal control patients and 40 PE patients.

Diagnostic criteria for patients with preeclampsia were strictly followed as provided by The American College of Obstetricians and Gynecologists (ACOG, No. 222). Exclusion criteria included adverse life history (smoking and drinking), twin or multiple pregnancies, comorbidities (chronic hypertension, diabetes, heart disease, immune system diseases, tumors, acute and chronic hepatitis, acute and chronic kidney disease), complications (pregnancy combined with intrahepatic cholestasis, gestational diabetes mellitus), and fetal malformations. Normal pregnant women (without pregnancy complications or other complications) who were registered and delivered in our hospital during the same period were randomly selected as the control group.

To avoid sample degradation, the placental tissue was collected immediately after the delivery of the placenta. Multipoint collection was performed on the maternal side of the placenta, avoiding the large vascular and calcification area. Placental chorionic tissue samples were repeatedly rinsed with PBS. After the excess PBS was absorbed by gauze, a portion of the samples was fixed in 4% paraformaldehyde for histopathological staining and the other parts were labeled and immediately frozen at − 80 °C for subsequent analysis.

Cell culture and treatment

Human trophoblast cell lines (HTR-8/SVneo and JAR cells) were purchased from the National Collection of Authenticated Cell Cultures and cultured in RPMI-1640 medium (Gibco; Thermo Fisher Scientific Inc-CN) supplemented with 10% fetal bovine serum (Gibco; Thermo Fisher Scientific Inc-CN), 100 UI/mL penicillin, and 100 µg/mL streptomycin (Hyclone; Thermo Fisher Scientific Inc-CN), and placed in an incubator containing 5% CO_2 at 37 °C for static culture.

Primary extravillous trophoblasts (EVTs) (HUM-iCELL-e003) in first trimester were purchased from the iCell Bioscience Technology Co., LTD in Shanghai and cultured in primary chorionic trophoblast cell culture system (PriMed-iCELL-045), and placed in an incubator containing 5% CO_2 at 37 °C for static culture.

Antisense oligonucleotide (ASO) against DUXAP8 (75 nm) (RiboBio Co., Ltd., Guangzhou, China), pcDNA3.1 plasmid with DUXAP8 (3 µg)/PCBP2 (3 µg)/FAM134B(3 µg), pcDNA3.1(+)-FAM134B-HA (3 µg) or pcDNA3.1(+)-FAM134B(mutLIR)-HA (3 µg), small interfering RNA against PCBP2 (50 nm) or FAM134B (50 nm) and their negative controls (si-NC, ASO-NC, pcDNA3.1) (Tsingke Biotechnology Co., Ltd., Beijing, China) were transfected using Lipofectamine 3000 (Invitrogen) based on the manufacturer's protocol.

ASO sequence of DUXAP8: ASO1#: AGTGTCTCAC TGGAGACTGA, ASO2#: CCAGCATTTGTGTCTCTTT T, ASO 3#: TGGAAATGTTCTGTGCAATC, ASO4#: GA AGTCCACAGATATGCAAC; siRNA sequence of PCBP2 protein: siRNA-1: GCCAUCAUUGCUGGCAUU, siRNA-2: CGGAUUCAGUGGCAUUG-AATT; siRNA sequence of FAM134B: siRNA-1: GCAGAAUCAUGGAUGAAU UTT, siRNA-2: GAGGUAUCCUGGACUGAUATT. The overexpressed plasmid sequences for DUXAP8, PCBP2 and FAM134B were separately obtained by Ensembl Genome Brower and NCBI query. The coding region of FAM134B and the HA-tag at the C-end were amplified by PCR and inserted into the pcDNA3.1(+) vector to obtain pcDNA3.1(+)-FAM134B-HA (Tsingke Biotechnology Co., Ltd., Beijing, China). The LIR motif: DDFELL, which binds to LC3 on FAM134B, was replaced with alanine residues: AAAAAA, which was obtained by a point mutation in pcDNA3.1(+)-FAM134B(mutLIR)-HA.

Cell viability assay

The Counting Kit-8 (CCK-8) cell proliferation and cytotoxicity assay kit (CA1210, Solarbio, China) was used to assess the cell proliferation capacity based on the manufacturer's protocol. Cells were seeded into 96-well plates at a density of 3000 cells per well. The complete medium was replaced with 200 µl RPMI-l640 medium containing 20 µl of CCK-8 regent. After incubating for 2 h at 37 °C, the absorbance values were measured at 450 nm. Detection was done at 24, 48, 72, and 96 h.

Cell migration and invasion assays

Transwell inserts containing a polycarbonate membrane with 8.0 µm pores (Corning 3422, NY, USA) were used to assess cell migration and invasion. Matrigel matrix (100 µl, BD Biocoat, USA) was used to coat the bottom of the Transwell inserts (Matrigel and serum-free medium diluted at 1:5) and incubated at 37 °C for 30 min. The treated cells were seeded at a density of 1×10^5 cells for invasion. The

Transwell inserts for migration were uncoated and the density of the cells was half that of the invasion experiments. After 24 h, the cells were fixed in 4% paraformaldehyde fixed and stained with 1% crystal violet. Images were captured under a microscope.

Tube formation assay

Matrigel matrix (10 µl) at a standard concentration was added to an ibidi angiogenesis slide (ibidi, Germany) and incubated at 37 °C for 30 min. A 50 µl suspension of cells (containing 1×10^4 cells) was added to each well and incubated at 37 °C for 3 h. The cells were observed and images were captured under a microscope.

Flow cytometry

Treated cells were harvested using trypsin without EDTA and washed with PBS. 4% paraformaldehyde induced the apoptosis of cells in untreated group. Cells were stained with fluorescein isothiocyanate (FITC)-Annexin V and propidium iodide (PI) or 15 min at room temperature according to the manufacturer's introduction of the Annexin V/FITC Apoptosis Detection Kit (BD Biocoat, USA). The cells were subject to flow cytometry (Beckman Coulter F500, CytoFLEX S, United States) and analyzed using CellQuest software (BD Biosciences). Double dispersion plots were drawn and divided into four quadrants including living, necrotic, early apoptotic and late apoptotic cells. The results are presented as the percentage relative to controls.

RNA isolation and quantitative real-time PCR (RT-qPCR)

Total RNA was extracted from placental tissues and cultured cells using the Non-chloroform RNA extraction kit (Bio Teke, China) according to the manufacturer's instructions. cDNA was synthesized using the PrimeScript^{TM}RT reagent Kit with gDNA Eraser (Takara, Japan). Quantitative RT-PCR was performed using the ChamQ Universal SYBR qPCR Master Mix (Vazyme, China) and analyzed on a LightCycler® 480 Fluorescence quantification system (Roche, Swiss). U6 and β-actin genes were used to normalize the relative expression of target genes with the $^{\triangle\triangle}$CT method. Primers for lncRNA and mRNA expression are listed in Table S1.

Nuclear-cytoplasmic fractionation

The nucleus and cytoplasm of HTR-8/SVneo and JAR cells were isolated using the Ambion® PAARIS™ Kit (AM1921, Life Technologies, USA). RNA was extracted for qRT-PCR. U6 and β-actin were used as markers for the nucleus and cytoplasm, respectively.

Western blot analysis

The placental tissues and treated cells were lysed in RIPA buffer with protease and phosphatase inhibitor cocktails (MedChemExpress, USA). Protein concentrations were measured using the BCA Protein Assay Kit (Beyotime, Shanghai, China). The protein samples were subjected to SDS-polyacrylamide gel electrophoresis, transferred to PVDF membranes (Bio-Rad, USA), followed by blocking in 5% nonfat milk for 2 h at room temperature. The membranes were incubated overnight at 4 °C with the following primary antibodies: mTOR (1:1000; 2972 S, CST), p-mTOR-s2448 (1:1000; 5536 S, CST), AKT (1:1000; 9272, CST), p-AKT-Ser473 (1:1000; AP1208, Abclonal), p-AKT-Thr308, (1:1000; AP1172, Abclonal), LC3 (1:1000; ab192890, Abcam), P62 (1:1000; ab109012, Abcam), Beclin-1 (1:1000; A7353, Abclonal), PCBP2 (1:1000; ab184962, Abcam), FAM134B (1:1000; ab151755,Abcam), β-actin (1:10000; AC004, Abclonal). The membranes were washed with TBST and incubated with secondary antibodies for 1 h at room temperature, which included HRP goat anti-rabbit IgG (H + L) (1:50000; AS014, Abclonal) or anti-mouse IgG (H + L) (1:50000; AS003, Abclonal). The protein signals were visualized by the Enhanced ECL chemiluminescent substrate kit (36222ES60, Yeasen, Shanghai).

RNA pull-down assay

Desthiobiotin-labeled RNAs were obtained using the Thermo Scientific Pierce RNA 3' Desthiobiotinylation Kit (20163, Thermo Fisher Scientific, USA) based on the manufacturer's protocol. The 3'-terminal of single-stranded RNA was labeled with T4 RNA ligase and used as a probe or target for protein-RNA interaction experiments. Using the Thermo Scientific Pierce Magnetic RNA–Protein Pull-Down Kit (20164, Thermo Fisher Scientific, USA), 50 pmol of labeled RNAs were mixed with 50 µl of streptavidin magnetic beads upside down for 30 min at room temperature. Total cell lysates (protein conc. >2 mg/mL) were added to each binding reaction and then the mixture was incubated for 60 min at 4 °C with agitation or rotation. After washing thoroughly three times, the RNA–protein bound beads were boiled for 5–10 min in SDS-PAGE buffer or nuclease-free water and the eluted proteins were detected by western blot analysis or mass spectrometry.

RNA immunoprecipitation (RIP)

To examine the binding capacity between protein and DUXAP8, an RNA immunoprecipitation (RIP) assay was performed using the Magna Binding Protein Immunoprecipitation kit (Millipore, MA, USA) according to the manufacturer's instructions. HTR-8/SVneo cells were lysed in RIP buffer containing a protease inhibitor cocktail and RNase inhibitor. Then, 50 µl protein A/G magnetic beads were washed with RIP buffer and incubated with 5 µg of anti-PCBP2/anti-PCBP1/anti-ANXA2 or anti-immunoglobulin G (anti-IgG; negative control) per reaction for 30 min at room temperature. The cell lysates were added to the Magnetic bead-antibody complex and the input sample was retained as a positive control. The mixtures and input sample were incubated for 30 min at 55 °C with rotation after adding proteinase K buffer solution. Finally, RNA was purified and resuspended in RNA-free water.

Fluorescent in situ hybridization (FISH)

The Ribo™ lncRNA FISH Probe for DUXAP8 and DUXAP8Ribo™ Fluorescent in Situ Hybridization Kit (R11060.0, Ribo, China) were obtained for RNA FISH. Cell climbing slices of HTR-8/SVneo and JAR cells were fixed in 4% paraformaldehyde for 10 min and permeabilized with 0.5% Triton X-100 in PBS for 5 min. Under dark conditions, 100 µL of probe hybridization solution containing 2.5 µL 20 µM FISH Probe Mix storage solution or internal reference FISH Probe Mix storage solution was added and hybridized overnight at 37 °C. After washing the cells with hybrid solution I, II, and III, the cells were stained with DAPI for 10 min. The climbing slices were fixed on glass slides and fluorescence detection was done using confocal microscopy (Olympus FV3000, Japan).

Immunofluorescence co-staining

Trophoblast cells (HTR-8/SVneo and JAR cells) were grown on cell climbing slices and after each experiment, the slices were fixed with freshly prepared 4% paraformaldehyde for 15 min and permeabilized with 0.5% Triton X-100 in PBS for 15 min. The deparaffinized paraffin Sect. (5 µm) of placental tissues were immersed in citrate buffer (0.01 M, pH 6.0) and antigen retrieval of the sections was performed by heating in a water bath. Subsequently, the slices and sections were blocked in 2% BSA for 30 min at room temperature and stained overnight at 4 °C with primary antibodies against FAM134B (1:50; PA5-113800, Invitrogen), LC3 (1:50; ab192890/ ab243506, Abcam), HA-Tag rabbit mAb (1:50;3724, CST), and mouse anti-HA-Tag mAb (1:50; AE008, Abclonal). The slices and sections were then washed in TBST buffer and incubated with FITC-labeled goat anti-rabbit IgG (1:100; AS011, Abclonal) or FITC-labeled goat anti-mouse IgG (1:100; AS001, Abclonal) for 1 h (1:200, Abclonal) in the dark. Finally, each sample was washed three times and incubated with DAPI solution for 5 min. Fluorescence signals were captured using an Olympus FV3000 microscope (Olympus, Japan).

Transmission electron microscopy (TEM)

Human placental tissues and trophoblast cell lines (HTR-8/SVneo and JAR cells) were fixed with 3% glutaraldehyde and post-fixed in 1% osmium tetroxide. After dehydrating in a series acetone and infiltrated with Epox 812, the semi-thin sections were stained with methylene blue and the ultra-thin sections were cut and stained with uranyl acetate and lead citrate. The sections were observed under a JEM-1400-FLASH Transmission Electron Microscope (JEOL, Japan).

Co-immunoprecipitation (Co-IP)

The treated trophoblast cell lines (HTR-8/SVneo and JAR cells) were lysed with RIPA buffer containing a protease inhibitor mixture (0.5 µl/100 µl) and ribonuclease inhibitors (0.25 µl/100 µl). The protein A/G magnetic beads (HY-K0202, MCE, USA) were incubated at 4 °C for 2 h after adding 400 µl diluted antibody (Ab) and then mixed with the antigen (Ag) sample (400 µl binding/washing buffer containing 5–50 µg of antigen) and incubated at 4 °C for 2 h. The Magbeads-Ab-Ag complex was washed with binding/wash buffer 5 times and eluted at 98 °C for 8 min after adding 25–50 µl of 1× SDS-PAGE loading buffer. The final solution was used for SDS-PAGE gel electrophoresis and western blot analysis was done to measure the expression level of the binding protein.

Detection of aggregated proteins

The trophoblast cells (HTR-8/SVneo and JAR cells) were plated on cell climbing slices. After transfection with ASO against DUXAP8 or pcDNA3.1 plasmid with DUXAP8, the cells were cultured with complete RPMI-1640 medium without penicillin-streptomycin for 48 h. To detect aggregated protein, the slices were fixed with 4% paraformaldehyde for 15 min and stained with Dual detection reagent from the ProteoStat Aggresome Detection Kit (ENZO, ENZ-51023-KP002, Farmingdale, NY, USA) based on the manufacturer's instruction. Moreover, the placental sections of animals first needed to be deparaffinized and then treated with 0.1% Sudan Black B for 20 min at room temperature. After fixed with 4% paraformaldehyde for 15 min, the sections were stained with ProteoStat dye for 15 min. Then,

the slices were incubated in DAPI solution for 5 min. Fluorescence images were captured using an Olympus FV3000 (Olympus, Japan).

RNA sequencing

Five pairs of placental tissues from normotensive pregnancy and PE patients were subject to full transcriptome sequencing (commissioned to Shanghai OE Biotech Co., Ltd.). The clinical information of the selected pregnant women was listed in Table S2.

Three different batches of HTR8-8/SVneo cells were transfected with pcDNA3.1 plasmid and DUXAP8 (3 μg) for 24 h and RNA was extracted for UID RNA sequencing (commissioned to SEQHEALTH Technology Co., LTD, China). The library products corresponding to 200–500 bps were enriched, quantified and finally sequenced on Novaseq 6000 sequencer (Illumina) with PE150 model. Raw sequencing data was first filtered by Trimmomatic (version 0.36), and clean reads were first clustered according to the UMI sequences, in which reads with the same UMI sequence were grouped into the same cluster. The de-duplicated consensus sequences were used for standard RNA-seq analysis. They were mapped to the reference genome of Homo_sapiens. GRCh38 using STAR software (version 2.5.3a) with default parameters. Reads mapped to the exon regions of each gene were counted by featureCounts (Subread-1.5.1; Bioconductor) and then RPKM was calculated. Genes differentially expressed between groups were identified using the edgeR package (version 3.12.1). Gene ontology (GO) analysis and Kyoto encyclopedia of genes and genomes (KEGG) enrichment analysis for differentially expressed genes were both implemented by KOBAS software (version: 2.1.1).

In vivo animal experiments

The animal experiments were performed in the Laboratory Animal Center of West China Second Hospital of Sichuan University (Chengdu, China), in which they adhered to the National Institutes of Health Guidelines on the Care and Use of Laboratory Animals and approved by the Ethics Committee on the Use of Animals of West China Second Hospital of Sichuan University (permit number: 2021-020). All animals were purchased from Chengdu Dossy Experimental Animals CO., LTD (Chengdu, China).

Specific pathogen-free SD rats [license number: SCXK (Chuan) 2020-0030] weighing 250 ± 20 g (males) and 250 ± 20 g (females) were purchased from Chengdu Dossy Experimental Animals CO., LTD. All rats were maintained on a low salt rodent chow diet with access to water ad libitum in a 12-h light-dark cycle. Timed breeding was performed and a vaginal swab was marked as gestational day 0.5 (GD 0.5).

Both pregnant and non-pregnant rats were randomly divided into four groups ($n = 6$ per group): normal saline (NS) group, Ad-EGFP group, Ad-sFlt-1 group, and Ad-DUXAP8-EGFP group (Hanbio Technology Co., Ltd). A previous study designated GD7.5–11.5 as the critical time window for uterine spiral artery remodeling after embryo implantation in rats [32]. Thus, GD9.5 pregnant rats were selected for tail vein injection of adenovirus or NS in this study. Next, 2×10^9 PFU adenovirus was injected into the tail vein of rats on GD9.5 for each group. The same volume of normal saline was injected into the normal saline group. The weight of rats was weighed, and systolic blood pressure was measured by a non-invasive blood pressure measurement system on GD9.5 and GD15(BP-98 A, Softron, Japan); Meanwhile, the rats were placed in individual metabolic cages to collect 24-hour urine samples at different time points (GD9, GD15 and GD19). Urine was frozen at − 80 °C and urinary albumin was detected using a protein assay kit (Yeasen, China) according to the manufacturer's instructions.

When the rats were anesthetized by inhaling isoflurane (2%) to reach a deep sleep, muscle relaxation, and stable breathing state, invasive blood pressure was measured by carotid intubation in the rats on GD19, and then rats were euthanized with 5% isoflurane for 5 min to collect the samples, including serum, placenta, the fetal rats, kidney, and liver. Placental and fetal weights were measured. The fetal rats per litter were counted and measured in length. Serum and part of tissues were immediately frozen at -80°C, and part of tissues was stored in 4% formaldehyde for morphological analysis and *immunohistochemistry staining*. The expression of DUXAP8 in placental tissues was determined by RT-qPCR. Western blotting was used to analysis the protein expression of AKT, p-AKT^{Ser473}, mTOR, p-mTOR^{S2248}, LC3II/LC3I and FAM134B (1:1000, HA721752, HUABIO) in placental tissues. The ProteoStat Aggresome Detection Kit was used to detect aggregated protein in Placental trophoblast cells. The levels of serum sFlt-1 and PlGF were measured by ELISA kit (Meimian, China) following the protocol.

Statistical analysis

SPSS 23 (SPSS Science Inc., Chicago, Illinois, USA) and GraphPad Prism (Version 8.3, GraphPad Software, La Jolla, CA, USA) were used for statistical analysis and figures were generated. The Kolmogorov-Smirnov test was used to assess the normality distribution of the data, and two independent sample t-tests was used to analyze the differences between the two groups. The non-parametric Mann–Whitney U test

was used if the data did not conform to a normal distribution. The correlation between two variables was analyzed using Pearson's correlation analysis. For data involving more than two groups, Multiple t test, one-way analysis of variance (ANOVA) and Tukey's test or two-way ANOVA were used for comparison. Data are presented as three independent experiments. Statistical significance was set at P values < 0.05.

Results

LncRNA DUXAP8 is upregulated in preeclamptic placental tissues

Whole transcriptome sequencing identified 976 differentially expressed lncRNA genes with 530 in the upregulated group (fold change > 2, $p < 0.05$) and 446 in the downregulated group (fold change < 0.5, $p < 0.05$) (Fig. 1A and B).Three up-regulated genes (DUXAP8, XLOC_011123, LOC105373022) (screening criteria: $1000 <$ length < 2000, pValue < 0.01, fold change > 2, and the average FPKM of at least one group in the two samples was > 3) and three downregulated genes (LINC02434, AP010595.1, AC009754.1) (screening criteria: $1000 <$ length < 2000,pValue < 0.01, fold change < 0.5, the average FPKM of at least one group > 1) among the top differentially expressed lncRNAs (Table S3) were further chosen. The RT-qPCR results in placental tissues of the PE and normal control groups for five lncRNAs (DUXAP8, XLOC_011123, LOC105373022, LINC02434, and AC009754.1) were consistent with those from whole transcriptome sequencing ($P < 0.05$), resulting in a concordance rate of 83.3% (5/6), and the difference in the expression level of DUXAP8 was the most obvious (Fig. S1 A). RT-qPCR ($n = 46$ in CTR group, $n = 40$ in PE group) confirmed that DUXAP8 expression was significantly increased in placentae of the PE group ($P < 0.001$, Fig. 1C). RNA-FISH indicated that DUXAP8 was primarily expressed in trophoblast layer of the microvilli in the placental tissue, and the red fluorescence of DUXAP8 in placentae of PE group was markedly enhanced than that of CTR group (Fig. 1D).

The clinical characteristics of the participants ($n = 46$ in the CTR group and $n = 40$ in the PE group) are listed in Table S4. Significant differences were noted in blood pressure, urinary protein levels, functional markers of the liver and kidney, fetal birth weight, body mass index (BMI) and gestational age between the two groups. A binary logistic regression analysis was conducted to determine the influence of BMI and gestational age on the expression level of DUXAP8. After adjusting the OR value, DUXAP8 expression remained markedly higher in the placental tissues of the PE group than that of control group (**Table S5**). The correlation between DUXAP8 expression and clinical indicators was analyzed and is shown in **Table S6**. The DUXAP8 levels were significantly and positively correlated with systolic blood pressure (SBP; $r = 0.8304$, $P = 0.0001$), lactate dehydrogenase (LDH; $r = 0.4953$, $P = 0.0012$) and Total bilirubin ($r = 0.3471$, $P = 0.0282$), but negatively correlated with Birth weight (r = -0.3152, $P = 0.0475$) and Birth length (r =-0.3250, $P = 0.0407$).

Upregulation of DUXAP8 inhibits the proliferation, migration, and invasion of trophoblasts

RT-qPCR of cytoplasmic and nuclear RNA isolated from the two cell lines (HTR-8/SVneo and JAR cells) indicated that the expression percentage of DUXAP8 in the nucleus was significantly higher than that in the cytoplasm (Fig. 1E-F). RNA-FISH revealed that DUXAP8 was primarily expressed in the nuclei of HTR-8/SVneo and JAR cells (Fig. 1E-F).

Four different antisense oligonucleotides (ASOs) against DUXAP8 (1#, 2#, 3#, and 4#) or the pcDNA3.1 plasmid with DUXAP8 were transfected into HTR-8/SVneo and JAR cells to knockdown or overexpress DUXAP8. As shown in Fig.S1B, ASO-DUXAP8-3# and ASO-DUXAP8-4# were both demonstrated to have robust effects in knocking down DUXAP8 in both cell lines, and was thus used for subsequent experiments. The results of the cell function experiments showed that increased DUXAP8 expression inhibited the proliferation, migration, and invasion of HTR-8/SVneo and JAR cells, whereas decreased DUXAP8 expression through transfection of ASO-DUXAP8-3# and ASO-DUXAP8-4# both exerted the opposite effects (Fig. 2A-D). However, the expression level of DUXAP8 had no influence on the apoptosis or tube formation of HTR-8/SVneo and JAR cells (Fig. S1 C-D).

Additionally, RNA-FISH and RT-qPCR of cytoplasmic and nuclear RNA also revealed that DUXAP8 was primarily expressed in the nuclei of primary EVT cells (Figure S2A). The functional experiments were then performed in primary EVT cells through knockdown and overexpression of DUXAP8, and we observed the same experimental results (Figure S2B-C).

DUXAP8 specifically binds to PCBP2 and affects its ubiquitination-mediated degradation

The functions of most lncRNAs located in the nucleus are mainly mediated by lncRNA-protein interactions. LncRNAs exert diverse functions by forming RNA-protein complexes, such as chromosome regulatory complexes, transcription factors and RNP complexes [33]. The RNA-protein binding solution obtained in the pull-down experiment was analyzed using gel electrophoresis and silver staining, and the results

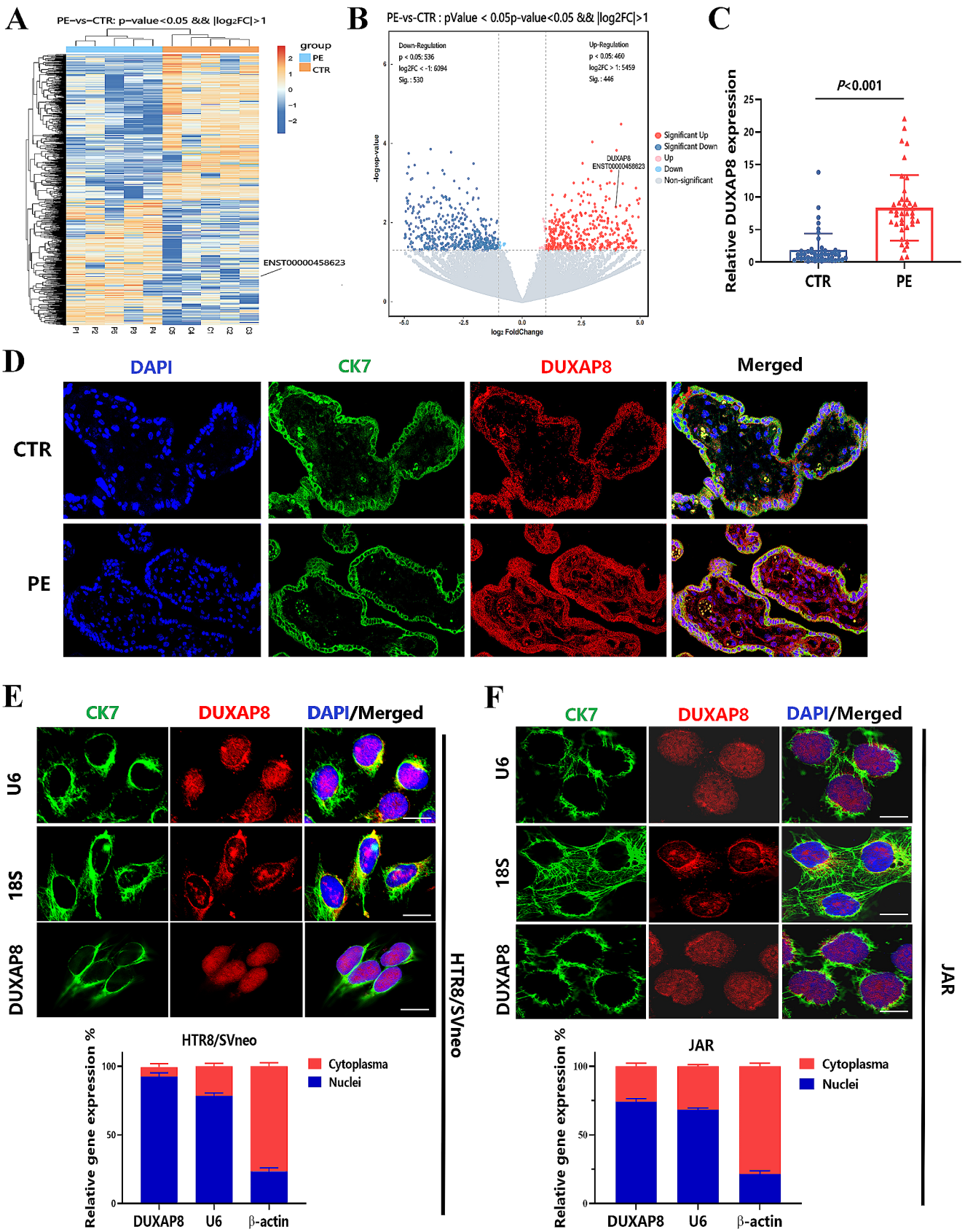
A
PE-vs-CTR: p-value<0.05 && |log2FC|>1
group
PE
CTR
ENST00000458623
B
PE-vs-CTR : pValue < 0.05p-value<0.05 && |log2FC|>1
Down-Regulation
p < 0.05: 536
log2FC < -1: 6094
Sig.: 530
Up-Regulation
p < 0.05: 460
log2FC > 1: 5459
Sig.: 446
DUXAP8
ENST00000458623
Significant Up
Significant Down
Up
Down
Non-significant
-log10p-value
log2 FoldChange
C
P<0.001
Relative DUXAP8 expression
CTR
PE
D
DAPI
CK7
DUXAP8
Merged
CTR
PE
E
CK7
DUXAP8
DAPI/Merged
U6
18S
DUXAP8
HTR8/SVneo
HTR8/SVneo
Relative gene expression %
Cytoplasma
Nuclei
DUXAP8
U6
β-actin
F
CK7
DUXAP8
DAPI/Merged
U6
18S
DUXAP8
JAR
JAR
Relative gene expression %
Cytoplasma
Nuclei
DUXAP8
U6
β-actin

Fig. 1 DUXAP8 expression is increased in preeclamptic placentae and primarily located in the nucleus of HTR-8/SVneo and JAR cells. **A-B** Heat map and volcano plot of the most differentially expressed lncRNAs in the placental tissues between the PE ($n=5$, preeclampsia) and CTR ($n=5$, normal control) group. **C** Validated expression of DUXAP8 in placentae of PE ($n=40$) and CTR ($n=46$) group was detected by RT-qPCR. Data are presented as the mean ± SEM, and statistical significance was evaluated using *t*-test for 2 comparisons. **D** The distribution and expression of DUXAP8 in the placental villi of CTR and PE group were detected by RNA-FISH (scar bar = 50 μm) (DAPI: nucleus; CK7: Cytokeratin 7, trophoblast marker protein). **E-F** Intracellular localization of DUXAP8 in HTR8/SVneo and JAR cells was observed by RNA-FISH (scar bar = 10 μm) (U6: nuclear marker; 18 S/β-actin: cytoplasmic marker) and cell fractionation assays ($n=3$, Data are presented as the percentage)

showed that protein binding to DUXP8 was mainly located at approximately 38KDa (Fig. 3A). Mass spectrometry results suggested that 77 proteins might bind to DUXAP8, but only 66 were specific, and the other 11 proteins might bind to multiple RNAs (Fig. 3A). Among them, three proteins (PCBP2, PCBP1, ANXA2) had a size of approximately about 38KDa (Fig. 3A). RNA-RIP revealed that the expression level of DUXAP8 bound to the PCBP2 protein was the highest, and the difference was significant compared with that of the IgG group (Fig. 3B), suggesting that the PCBP2 protein exhibited the strongest binding ability and the highest specificity for DUXAP8. In addition, western blot analysis showed that the protein expression of PCBP2 in the RNA–protein binding solution obtained in the pull-down experiment was substantially high (Fig. 3C).

After transfecting HTR-8/SVneo and JAR cells with pcDNA3.1 plasmid with DUXAP8 or ASO-DUXAP8-4#, western blot analysis showed that DUXAP8 overexpression increased the protein expression of PCBP2 (Fig. 3D), or the opposite. In addition, the protein expression of PCBP2 in the placental tissues of PE patients was higher than that in normal controls (Fig. 3E). RT-qPCR revealed that PCBP2 mRNA levels were not affected by DUXAP8 expression (Fig. 3F). These results suggest that DUXAP8 binding to PCBP2 protein do not affect its mRNA expression level, but only its protein levels.

PCBP2 protein is degraded via the ubiquitination degradation pathway [34]. Therefore, we hypothesized that DUXAP8 may affects the ubiquitination and degradation of PCBP2 and alters its expression. Western blot analysis revealed that PCBP2 expression in the ASO-DUXAP8-4#+MG132 (proteasome inhibitor) group was substantially increased than that in the ASO-DUXAP8-4# group, indicating that the observed decrease in PCBP2 protein levels following DUXAP8 knockdown was indeed related to an increase in ubiquitin-mediated degradation (Fig. 3G). The effect of ubiquitination varies according to the location of the ubiquitin molecule (Ub), of which Lys48 (K48) is the most common site associated with substrate degradation [35]. A co-immunoprecipitation (CO-IP) assay revealed that the overall Ub and K48-UB levels in the PCBP2 protein were significantly increased in the ASO-DUXAP8-4# group (Fig. 3H), suggesting that DUXAP8 knockdown promoted K48 ubiquitination of PCBP2 and its degradation via ubiquitination.

Upregulation of DUXAP8 increases the phosphorylation of the AKT/mTOR signaling pathway and decreases autophagy levels of trophoblast cells

To further explore the downstream mechanisms underlying the regulatory effects of DUXAP8 on the behavior of trophoblastic cells, HTR8-8/SVneo cells were transfected with pcDNA3.1 plasmid containing DUXAP8, and RNA was extracted for UID RNA sequencing. GO and KEGG analyses suggested that the differentially expressed genes were closely related to the assembly and regulation of autophagy, whereas the phosphatidylinositol signaling system and mTOR signaling pathway may also be involved (Fig. 4A).

Western blotting analysis indicated a significant increase in the expression of p-AKT^{Ser473} and p-mTOR^{S2248} in the DUXAP8 overexpression group of HTR-8/SVneo and JAR cells, whereas DUXAP8 knockdown decreased the expression of p-AKT^{Ser473} and p-mTOR^{S2248} (Fig. 4B). Transmission electron microscopy (TEM) and western blot analysis revealed that DUXAP8 overexpression downregulated the number of autolysosomal vacuoles and the ratio of autophagy protein LC3-II/LC3-I and upregulated P62 expression in HTR-8/SVneo and JAR cells (Fig. 4C-F). Conversely, DUXAP8 knockdown increased the number of autolysosomes and the LC3-II/LC3-I ratio, while decreasing P62 expression. However, the expression level of DUXAP8 had no influence on the Beclin-1 expression. In addition, the expression of p-AKT^{Ser473} and p-mTOR^{S2248} increased, and the ratio of the autophagy protein LC3-II/LC3-I decreased in the preeclamptic placentae (Fig. S3A).

Following co-transfection of the pcDNA3.1 plasmid with DUXAP8 and PCBP2 siRNA, decreased levels of PCBP2 inhibited the activation effect of DUXAP8 overexpression on phosphorylation of the AKT/mTOR signaling pathway (Fig. S3B). Following co-transfection of ASO-DUXAP8-4# and pcDNA3.1 plasmid with PCBP2, PCBP2 overexpression enhanced the phosphorylation of the AKT/mTOR signaling pathway (Fig. S3C).

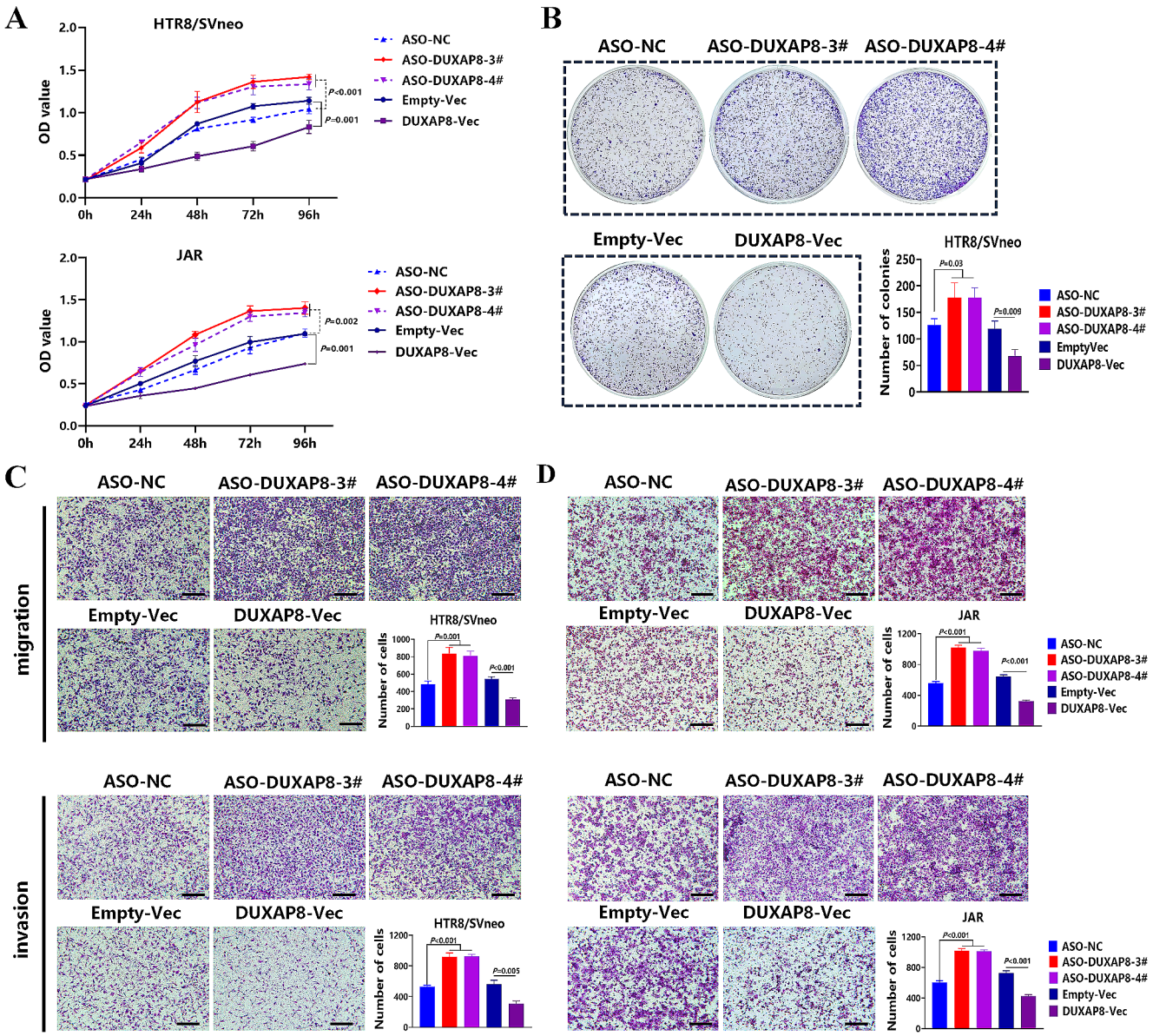

Fig. 2 Overexpression of DUXAP8 inhibits the proliferation, migration, and invasion of HTR-8/SVneo and JAR cells. **A-B** The effects of knockdown or overexpression of DUXAP8 on the proliferation of HTR-8/SVneo cells and JAR cells as detected by CCK-8 ($n=3$) and colony formation assays ($n=3$). **C-D** The effects of knockdown or overexpression of DUXAP8 on the migration and invasion ability of HTR-8/SVneo (**C**) and JAR cells (**D**) as detected by Transwell assay (without or with Matrigel) ($n=3$, scar bar = 100 μm). Data are presented as the mean ± SD, statistical significance was evaluated using the *t*-test or Mann-Whitney U for 2 comparisons, one-way ANOVA and Tukey test or two-way ANOVA for multiple comparison vs. negative control

DUXAP8 overexpression decreases FAM134B-mediated ER-phagy in trophoblast cells by activating the AKT/mTOR signaling pathway

Compared with the CTR group (the ER showed elongated structure), TEM revealed that the ER was obviously swollen, and accumulated in the cytoplasm of the placental villus trophoblastic cells of PE patient, which also contained floccules with medium electron density (Fig. 5A). The structure of the swollen ER was clearly observed in autophagosomes. Similarly, the accumulation of lytic ER fragments was observed in HTR-8/SVneo trophoblasts overexpressing DUXAP8(Fig. 5A). These results suggested that the clearance capacity of endoplasmic reticulum (ER) in pathological state is impaired.

Firstly, immunofluorescence co-staining indicated that the red fluorescence of FAM134B and the green fluorescence of LC3 were both significantly decreased in the DUXAP8 overexpression group (DUXAP8-Vec group), and the overlapping portions of the two fluorescent colors were

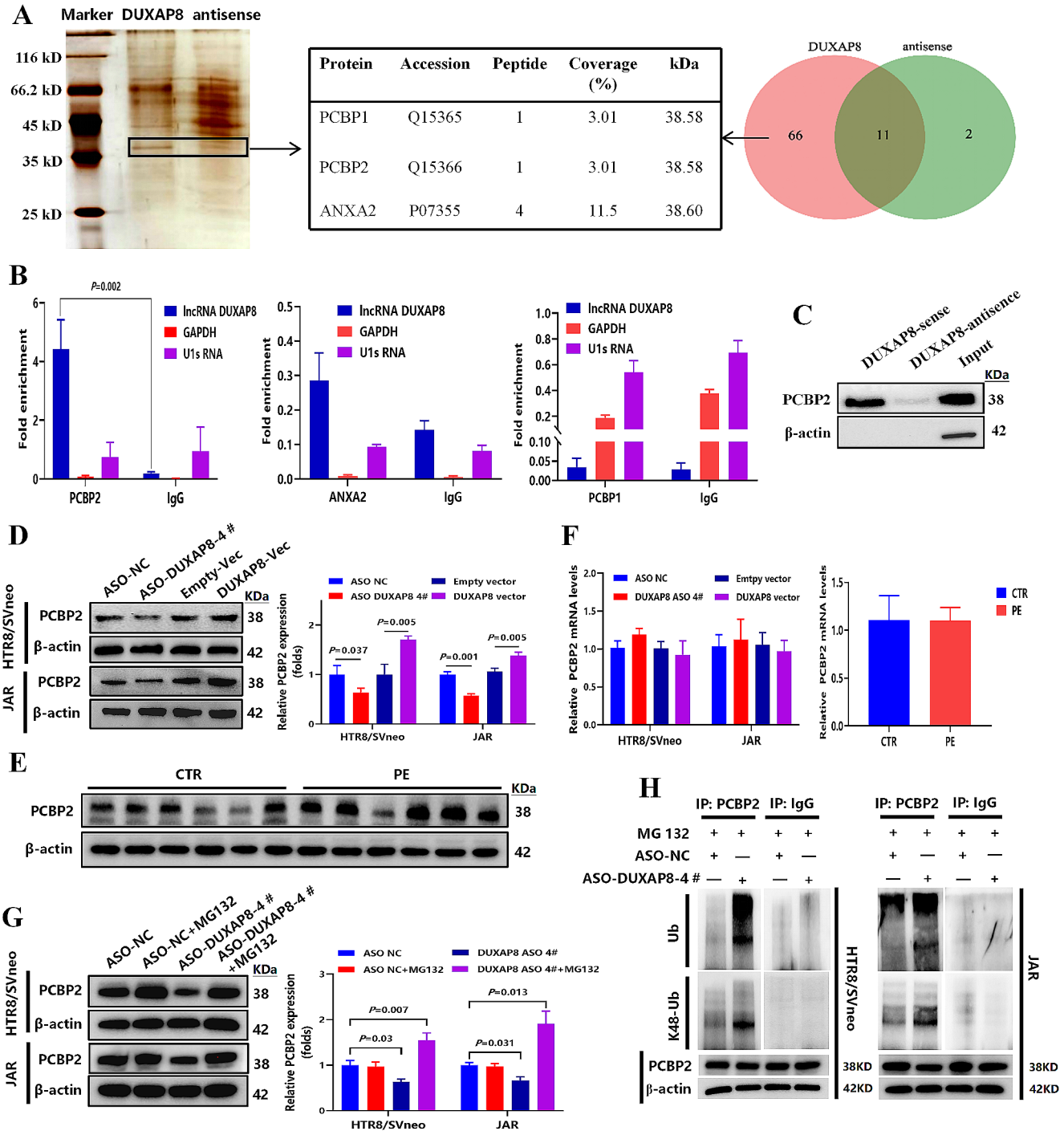

Fig. 3 DUXAP8 specifically binds to the PCBP2 protein and affects its ubiquitin-mediated degradation. The sense strand DUX (+) and antisense strand DUX (-) of DUXAP8 were transfected into HTR-8/SVneo cells. **A** Combined with the Mass spectrometry analysis of RNA–protein binding solution, three proteins (PCBP2, ANXA2, and PCBP1) corresponding to the band size in the silver staining of binding solution in the pull-down experiment. **B** RNA-RIP and RT-qPCR were used to verify protein specifically bound to DUXAP8 in HTR-8/SVneo cells ($n=3$). IgG: Negative control for RIP assay, GAPDH/U1sRNA: negative control for RT-qPCR analysis. **C** the expression of PCBP2 protein in the RNA–protein binding solution was detected by western blot. **D-F** The protein and mRNA expression of PCBP2 in HTR-8/SVneo and JAR cells after knockdown or overexpression of DUXAP8 ($n=3$) and placental tissues of CTR and PE group ($n=12$). CTR: normal control group; PE: Preeclampsia. **G** The expression level of PCBP2 protein between the ASO-DUXA8-4# group and ASO-DUXA8-4# +MG132 (proteasome inhibitor, 100nM) group ($n=3$). **H** PCBP2 ubiquitination levels were verified by Co-immunoprecipitation (Co-IP) after downregulation of DUXAP8 in HTR-8/SVneo and JAR cells. IgG: Co-IP negative control. Data are presented as the mean ± SD/SE, statistical significance was evaluated using the *t*-test or Mann-Whitney U for 2 comparisons

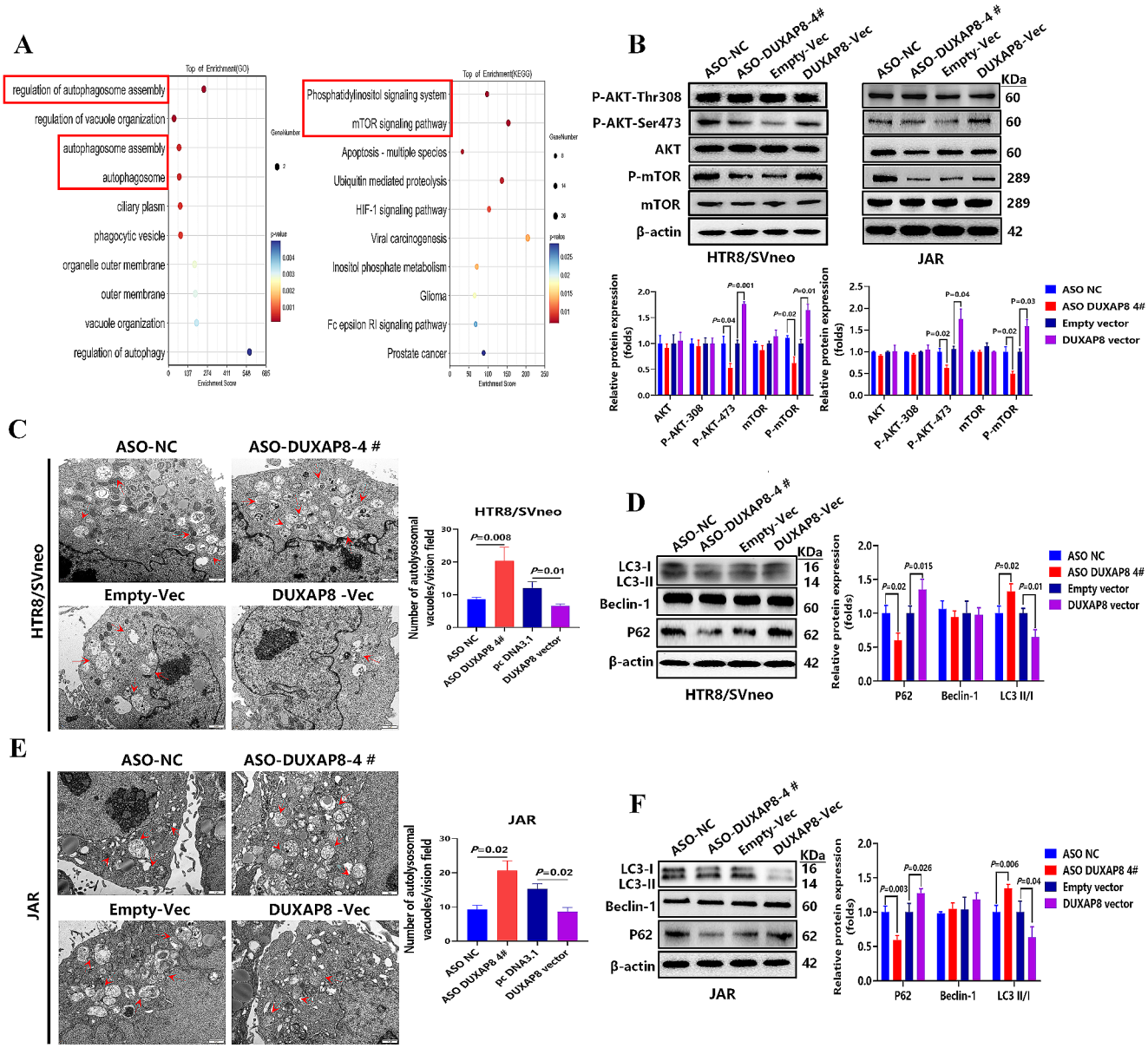

Fig. 4 DUXAP8 Overexpression increases the phosphorylation of the AKT/mTOR signaling pathway and decreases autophagy levels of trophoblast cells. **A** GO and KEGG analysis of differentially expressed genes identified by RNA sequencing. **B** the effects of knockdown or overexpression of DUXAP8 on the expression of key signaling proteins (AKT, mTOR, p-AKT^{Ser473}, p-AKT^{Thr308}, p-mTOR^{S2248}) in HTR-8/SVneo($n=3$) and JAR ($n=3$) cells were determined by western blot. **C-F** The effects of knockdown or overexpression of DUXAP8 on the autolysosomal vacuoles (6000×, red arrows: autolysosomes) or autophagy-related proteins (LC3-II/LC3-I, P62, Beclin-1) in HTR-8/SVneo and JAR cells were separately examined by transmission electron microscopy (TEM) ($n=3$) or western blot ($n=3$).Data are all presented as the mean ± SD, statistical significance was evaluated using the *t*-test or Mann-Whitney U for 2 comparisons

also significantly decreased (Fig. 5B). Moreover, western blotting results indicated a significant downregulation in the expression of FAM134B protein in the DUXAP8-Vec group, whereas decreased DUXAP8 expression (the ASO-DUXAP8-4# group) exerted the opposite effects (Fig. 5C). And FAM134B expression in the preeclamptic placentae was also decreased (Fig. S3A). Furthermore, compared with the ASO-DUXAP8-4# group, FAM134B expression was inversely decreased in the ASO-DUXAP8-4# + MHY1485 (agonist of the mTOR signaling pathway) group (Fig. 5D), indicating that activation of the mTOR signaling pathway mediates reduced expression of FAM134B protein. Taken together, these results suggest that overexpression of DUXAP8 mediates the decreased expression of FAM134B protein by activating mTOR signaling.

ER-phagy receptor proteins induce ER-phagy by interacting directly with LC3-II through the LC3-binding region (LIR). FAM134B contains a conserved LIR motif [24].

Therefore, we constructed an LIR motif wild-type recombinant plasmid (HA-FAM134B^{WT}) and an LIR motif mutant recombinant plasmid (DDFELL/AAAAAA; HA-FAM-134B^{LIRmut}), and transfected them into trophoblast cells. Fluorescence co-localization and Co-IP experiments confirmed that FAM134B bound to LC3 via the LIR motif. And after DUXAP8 knockdown, the level of LC3 protein binding to FAM134B significantly increased (Fig. 5E-F). The degree of binding was also significantly enhanced, and the yellow fluorescent spots significantly increased (Fig. 5E-F).

Moreover, protein aggregation was detected, and the results indicated that overexpression (knockdown) of DUXAP8 increased (decreased) protein aggregation in HTR-8/SVneo and JAR cells (Fig. 6A), which further confirmed that DUXAP8 overexpression impairs ER-phagy, which in turn, causes an increased accumulation of protein in HTR-8/SVneo and JAR cells.

FAM134B overexpression promotes the proliferation, migration, and invasion of trophoblast cells

We further explored the effect of ER-phagy on the biological behavior of trophoblasts. Overexpression of FAM134B alone with FAM-Vec can promote proliferation, migration and invasion of HTR-8/SVneo and JAR cells. And after co-transfection with DUXAP8-Vec and FAM-Vec, the increased level of FAM134B significantly reversed the inhibitory effect of DUXAP8 overexpression on the proliferation, migration, and invasion of trophoblasts (Fig. 6B-D), confirming that improved ER-phagy mediated by overexpression of FAM134B promotes the biological behavior of trophoblastic cells.

DUXAP8 overexpression induces preeclampsia-like phenotypes and impairs ER-phagy mediated by the AKT/mTOR signaling pathway in pregnant rats

To further verify whether the upregulation of DUXAP8 contributes to preeclampsia, we established a rat model of DUXAP8 overexpression by injecting Ad-DUXAP8-EGFP on gestational day 9.5 (GD9.5) into the tail vein (Fig. 7A). DUXAP8 expression in placental tissues of Ad-DUXAP8-EGFP group on GD19 was increased (Fig. 7B). Moreover, compared to the normal saline blank (NS) and Ad-EGFP groups, SBP and DBP (GD15, 19) in the Ad-DUXAP8-EGFP and Ad-sFlt1 groups were substantially increased (Fig. 7C).

Furthermore, DUXAP8 overexpression resulted in elevated 24-hour proteinuria levels (Fig. 7C). Typical preeclampsia-like phenotypes (blood pressure and 24-h proteinuria) were not induced by the upregulation of DUXAP8 in non-pregnant rats (Fig. S4A). The placental weights of rats in the Ad-DUXAP8-EGFP and Ad-sFlt-1 groups significantly decreased (Fig. 7D), and fibrous matrix deposits were identified using Masson's trichrome staining (Fig. 7E). Relevant studies and obstetric guidelines have confirmed that PlGF (placental growth factor), sFlt-1 (soluble fms-like tyrosine kinase 1), and the sFlt-1/PlGF ratio are key factors in predicting and diagnosing preeclampsia [36, 37]. Our results showed that the serum sFlt1/PlGF ratio increased in the Ad-sFlt1 group, and similar results were observed in the Ad-DUXAP8-EGFP group (Fig. S5A).

Although excessive sFlt-1 and DUXAP8 levels can lead to reduced fetal growth, including fetal weight loss and reduction in length, no differences in litter size were observed between the groups (Fig. S5B-C). Furthermore, histopathological analysis of renal tissues revealed glomerular swelling and mesangial hyperplasia (Fig. 7E). The HE staining revealed hepatic sinus stenosis and disordered surrounding hepatocytes (Fig. S5D). However, such damage to tissues did not occur in nonpregnant rats (Fig. S4B).

To further clarify the effect of DUXAP8 overexpression on AKT/mTOR signaling and ER-phagy, related indices were determined. Western blot analysis revealed that the expression levels of placental p-AKT^{Ser473} and p-mTOR^{S2248} were significantly increased in the Ad-sFlt1 and Ad-DUXAP8-EGFP groups, whereas the expression levels of LC3-II/LC3-I and FAM134B were markedly decreased (Fig. 7F).Fluorescence co-localization indicated that the red fluorescence of FAM134B and the green fluorescence of LC3 protein were both significantly decreased in the Ad-DUXAP8-EGFP group, and yellow fluorescent spots were also significantly decreased in both the Ad-sFlt1 and Ad-DUXAP8-EGFP groups (Fig. S5E). Moreover, the ProteoStat dye detection assay revealed increased protein aggregation in the Ad-sFlt1 and Ad-DUXAP8-EGFP groups (Fig. 7G). These results support our observations in PE placentae, HTR-8/SVneo and JAR cells that DUXAP8 overexpression mediates impaired ER-phagy, which in turn leads to the accumulation of protein aggregates.

Discussion

Numerous studies have explored the specific pathogenesis of PE, however, which still remains enigmatic and brings great challenges to the improvement of clinical management. It is widely accepted that insufficient trophoblast infiltration and spiral artery remodeling disorders during early pregnancy is the primary pathophysiology base of PE [1, 2]. In this study, we have reported a previously uncovered mechanism event in the pathogenesis of PE, ER-phagy, playing an important role in the aggregation of misfolded proteins. Firstly, we

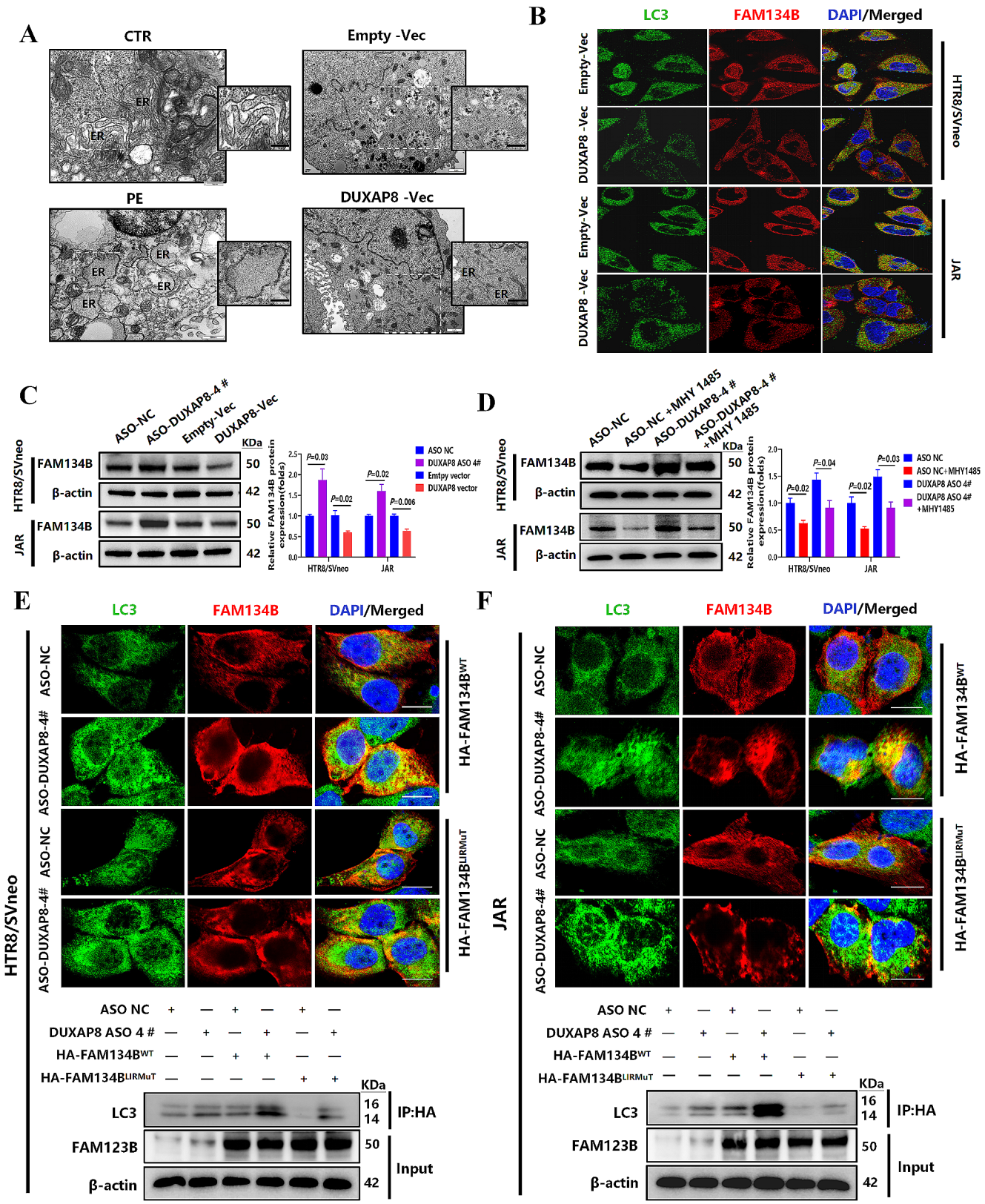
A
CTR
Empty -Vec
PE
DUXAP8 -Vec
ER
B
LC3
FAM134B
DAPI/Merged
Empty-Vec
DUXAP8 -Vec
HTR8/SVneo
JAR
C
ASO-NC
ASO-DUXAP8-4 #
Empty-Vec
DUXAP8-Vec
KDa
FAM134B
β-actin
50
42
Relative FAM134B protein expression(folds)
P=0.03
P=0.02
P=0.02
P=0.006
ASO NC
DUXAP8 ASO 4#
Emtpy vector
DUXAP8 vector
D
ASO-NC
ASO-NC +MHY 1485
ASO-DUXAP8-4 #
ASO-DUXAP8-4 #+MHY 1485
P=0.02
P=0.04
P=0.02
P=0.03
ASO NC
ASO NC+MHY1485
DUXAP8 ASO 4#
DUXAP8 ASO 4# +MHY1485
E
F
HTR8/SVneo
JAR
ASO-NC
ASO-DUXAP8-4#
HA-FAM134B^WT
HA-FAM134B^LIRMuT
ASO NC
DUXAP8 ASO 4 #
HA-FAM134B^WT
HA-FAM134B^LIRMuT
KDa
LC3
FAM123B
β-actin
16
14
50
42
IP:HA
Input

Fig. 5 DUXAP8 overexpression decreases FAM134B-mediated ER-phagy in trophoblast cells by activating AKT/mTOR signaling pathway. **A** Pathological changes of endoplasmic reticulum in villus trophoblastic cells of placentae from CTR and PE patients and HTR-8/SVneo cells with overexpressed DUXAP8 were observed by transmission electron microscopy (TEM). **B** Immunofluorescence analysis of the LC3 and FAM134B proteins in HTR-8/SVneo and JAR cells (Scale bar = 10 μm). **C** The effects of knockdown or overexpression of DUXAP8 on the expression of FAM134B were examined by western blot analysis ($n = 3$). **D** The expression of FAM134B protein in HTR-8/SVneo and JAR cells treated with ASO-DUXA8-4# and MHY1485 (mTOR agonist, 50 nM) was detected by western blot ($n = 3$). **E-F** After transfected with ASO-DUXA8-4# or ASO-NC in HTR-8/SVneo and JAR cells, immunofluorescence analysis of the co-localization of LC3 with WT or LIRmut HA-FAM134B (Scale bar = 5 μm) and Co-immunoprecipitation (Co-IP) assay was used to verify the interaction between WT or LIRmut HA-FAM134B and LC3. Data are all presented as the mean ± SD, statistical significance was evaluated using the *t*-test or Mann-Whitney U for 2 comparisons

found that lncRNA DUXAP8 expression was significantly upregulated in preeclamptic placentae. DUXAP8 specifically binds to PCBP2 and inhibits its ubiquitination-mediated degradation, and decreased levels of PCBP2 reversed the activation effect of DUXAP8 overexpression on AKT/mTOR signaling pathway. Secondly, Function experiments showed that DUXAP8 overexpression inhibited trophoblastic proliferation, migration, and invasion of HTR-8/SVneo and JAR cells. And pathological accumulation of swollen and lytic ER was observed in DUXAP8-overexpressed HTR8/SVneo cells and PE placental villus trophoblast cells, which suggesting that ER clearance ability is impaired. Further studies found that DUXAP8 overexpression impaired ER-phagy and caused protein aggregation medicated by reduced FAM134B and LC3II expression (key proteins involved in ER-phagy) via activating AKT/mTOR signaling pathway. The decreased level of FAM134B significantly inhibited the positive effect of DUXAP8 knockdown on the proliferation, migration, and invasion of trophoblasts. Moreover, DUXAP8 overexpression during the key period of placentation caused PE-like phenotypes in pregnant rats along with activated AKT/mTOR signaling, decreased expression of FAM134B and LC3-II proteins and increased protein aggregation in placental tissues.

DUXAP8 is a new type of pseudogene and many studies have demonstrated its role as a cancer gene. Its expression is associated with the proliferation, invasion, migration, and anti-autophagy of tumors [31]. For example, DUXAP8 inhibits miR-498 by activating the AKT/mTOR pathway mediated by TRIM44, thereby promoting proliferation, metastasis, and epithelial-mesenchymal transition in non-small cell lung cancer cells [38, 39]. In the present study, RNA-FISH revealed that DUXAP8 was primarily expressed in placental extravillous trophoblasts. Functional experiments subsequently verified that DUXAP8 overexpression significantly inhibited proliferation, migration, and invasion of trophoblasts. These results suggested that DUXAP8 may be involved in the pathogenesis of PE by altering the biological behavior of trophoblast cells. It is of note that a recently published paper presented contrasting findings, which indicating that DUXAP8 is downregulated in PE placenta and that knockdown of DUXAP8 inhibits proliferation and migration while increasing apoptosis in HTR-8/SVneo and JAR cells [40]. These conflicting results may be related to the incomplete equivalence of the factors influencing the study, such as different isoforms of lncRNA gene, differences in knockdown methods, data analysis and interpretation, different clinical samples included, and differences in placental tissue sampling and examined regions.

PCBP2 (Poly(rC)-binding Protein 2) is a heterogeneous nuclear ribonucleoprotein (hnRNP) that can specifically bind to RNA fragments rich in cytosine [41], and plays an important role in post-transcriptional and translational regulation [42]. It has also been mentioned that PCBP2 is closely related to the occurrence and progression of certain types of cancer, such as leukemia, glioma and gastric cancer [41]. PCBP2 may promote the promotion of miR-151-5p and miR-16 in glioma cell migration and invasion by reducing the function of ARHGDIA. Recently, it was found that after PCBP2 knockout, EVTs failed to differentiate into invasive phenotypes [43], which suggesting that PCBP2 may be an important regulator of EVTs differentiation into invasive phenotypes. Moreover, the result of RNA-seq performed on HTR-8/SVneo cells after PCBP2 knockout implicated that gene silencing of PCBP2 resulted in a large number of gene splicing disorders, which played an important role in cell growth, proliferation and cell cycle [43]. It has been reported that the expression of PCBP2 protein is regulated by ubiquitination, and PCBP2 can recruit the E3 ligase AIP4 containing the HECT domain to catalyze the polyubiquitination degradation of K48 junctions [34, 44]. In our study, it was confirmed that after downregulating DUXAP8 in trophoblast cells, the overall Ub and K48-Ub level of PCBP2 protein were both significantly increased, which indicating that DUXAP8 knockdown promoted K48 ubiquitination of PCBP2 and its degradation via ubiquitination. Moreover, the expression level of PCBP2 regulated the effect of DUXAP8 overexpression on AKT/mTOR signaling pathway.

There have been controversies regarding the alterations of autophagy in placenta of women with PE. Some researchers have detected defective autophagy in hypoxia-induced trophoblasts or placental tissues of PE patients [17, 18]. Nakashima et al. showed that defective autophagy inhibits invasion ability of trophoblast cells and may contribute to poor vascular remodeling [18].As the key markers of autophagy, the expression of LC3-II and beclin-1 are closely related to the activation of autophagy [45, 46]. Weel et al. have described decreased LC3-II and beclin-1 mRNA

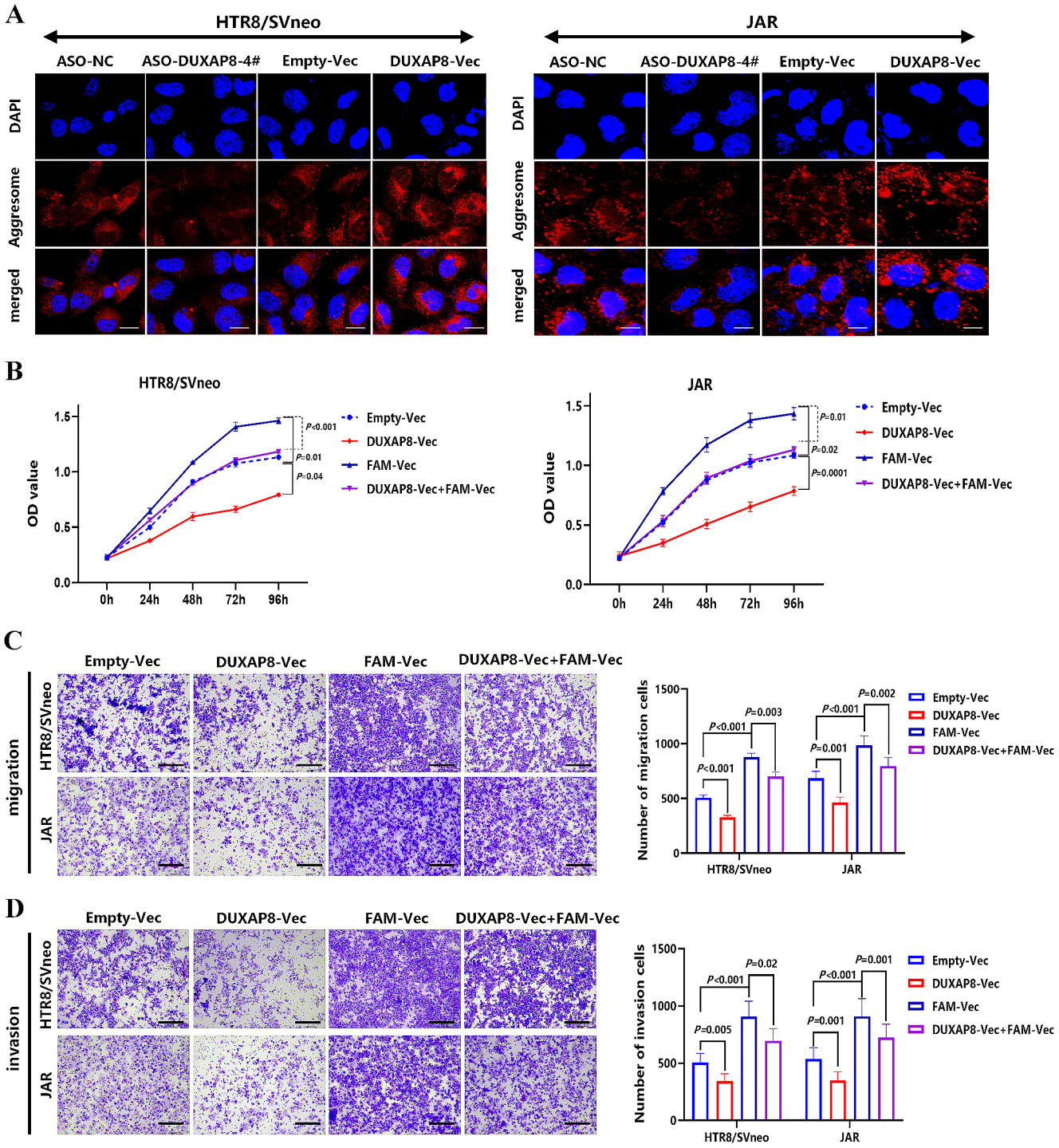

Fig. 6 Upregulation of FAM134B promotes the proliferation, migration, and invasion of HTR-8/SVneo and JAR cells. **A** The effects of knockdown or overexpression of DUXAP8 on intracellular protein aggregation in HTR-8/SVneo and JAR cells was detected by Protein Aggresome detection kit (Scale bar = 10 μm) (DAPI: nucleus; Aggresome: protein aggregates). **B-D** After co-transfecting with DUXAP8-Vec and FAM-Vec in HTR-8/SVneo ($n = 3$) and JAR ($n = 3$) cells, CCK-8 and Transwell assays (without or with Matrigel) were performed to detect proliferation, migration (scar bar = 100 μm), and invasion (scar bar = 100 μm) ability. Data are presented as the mean ± SD, statistical significance was evaluated using the *t*-test or Mann-Whitney U for 2 comparisons, one-way ANOVA and Tukey test or two-way ANOVA for multiple comparison

and protein expression in the PE placenta [45]. On the other hand, many other studies suggested that autophagy mechanisms not decreased in PE [46–49]. Akaishi and coworkers demonstrated upregulated LC3-II and down-regulated SQSTM1/p62(a widely studied autophagy substrate, negatively correlated with autophagy activity) in PE placenta [49].Oh et al. recently reported that inhibition of autophagy in vitro increases the invasion ability of extravillous trophoblast, in contrast with the results of Nakashima et al [46]. In our study, through RNA sequencing and various experimental methods, we found that DUXAP8 overexpression activated the phosphorylation of the AKT/mTOR signaling pathway and inhibited autophagy in trophoblast cells with decreased expression of LC3-II and downregulated number of autolysosomal vacuoles. Previous studies have indicated a close inverse correlation between mTORC1 activation and autophagy induction, with the initiation of autophagy accompanied by the inactivation of mTORC1 [50–52]. mTOR protein expression in the placental tissue of PE patients was negatively correlated with LC3-II protein expression [53]. These studies also suggested that the inhibition of autophagy may be one of the causes of PE pathogenesis.

The reduced efficiency of the autophagy mechanism has been associated with the accumulation of misfolded proteins [15, 16, 54]. Endoplasmic reticulum (ER) is the major intracellular organ for protein synthesis, folding and modification. Selective autophagy of the endoplasmic reticulum (ER-phagy) involves in the clearance of aggregated proteins and the resolution of abnormal ER, and influences the quality, quantity, and secretion of ER proteins [55, 56]. Surprisingly, we observed the accumulation of swollen and lysed ER in DUXAP8-overexpressing HTR-8/SVneo trophoblast cells and placental villus trophoblastic cells of PE patients, suggesting that ER clearance ability is impaired. Therefore, we hypothesized that DUXAP8 overexpression would impair ER-phagy. Our results further confirmed that knockdown of DUXAP8 significantly increased FAM134B expression and enhanced the degree of binding of FAM134B to LC3-II, ultimately promoting ER-phagy and protein aggregation in trophoblasts. Moreover, DUXAP8 was involved in the regulation of FAM134B expression through the mTOR signaling pathway. Activation of mTOR signaling inhibits FAM134B expression. Transcription factor EB (TFEB), a downstream target of mTORC1, regulates the FAM134B promoter through a DNA-regulatory binding site (CLEAR) and mutations at this site can eliminate the induction of ER-phagy [57, 58]. Phosphorylation of TFEB by mTORC1 inhibits its dephosphorylation and nuclear translocation, thereby reducing FAM134B expression [59]. This may be the downstream mechanism by which mTORC1 signaling affects FAM134B-mediated ER-phagy.

Current studies on ER-phagy-related diseases have primarily focused on nervous system diseases, viral infections, and cancer [60]. The dysfunction of ER-phagy has now been demonstrated to be involved in various neurodegenerative diseases [61], like Alzheimer's disease, Niemann-Pick Type C or Parkinson's can. FAM134B-mediated ER-phagy is associated with Niemann-Pick Type C disease, a fatal progressive neurodegenerative disease [26]. FAM134B functions as an oncogene or a tumor suppressor gene, which is involved in regulating various biological behaviors, such as the cell cycle and proliferation, and is closely associated with the PI3K/AKT signaling pathways [62, 63]. Our results indicate that the impairment of ER-phagy mediated by FAM134B downregulation inhibits the proliferation, migration, and invasion of trophoblasts, which may be involved in the pathogenesis of preeclampsia. FAM134B plays an important role in the development of diseases and may be a useful biomarker for disease screening and diagnosis or a target for the development of new therapies.

Previous studies have demonstrated that adenoviral overexpression of sFlt-1 or chronic administration of sFlt-1 in pregnant rats induces endothelial dysfunction, hypertension, proteinuria, and classical preeclampsia [64]. Therefore, to further clarify the role of DUXAP8 in the pathogenesis of PE through in vivo experiments, an adenovirus containing DUXAP8-overexpressing plasmid was injected into the tail veins of rats, and sFlt-1 overexpression in pregnant rats was used as a positive control. DUXAP8 overexpression induced typical PE-like phenotypes in vivo, activated the AKT/mTOR signaling pathway, decreased the expression of FAM134B and LC3-II proteins and increased protein aggregation in placental tissues.

In conclusion, our study revealed the important role of lncRNA DUXAP8 in regulating trophoblast biological behaviors through FAM134B-mediated ER-phagy and provided a new perspective for the pathogenesis of PE. DUXAP8 binds specifically to the PCBP2 protein, and decreased levels of PCBP2 significantly inhibited the activation effect of DUXAP8 overexpression on AKT/mTOR signaling pathway. However, the specific mechanism by which DUXAP8/PCBP2 regulates the AKT/mTOR signaling pathway requires further exploration. FAM134B plays an important role in the development of diseases and may be a useful biomarker for the screening and diagnosis of preeclampsia or possibly a target for the development of new therapies. Relevant studies of molecule and signaling pathways for further elucidating the pathogenesis of PE deserve further attention and seems likely to promote efforts to the development of novel early onset diagnostics and therapeutic targets for PE clinical management to improve maternal and infant prognosis.

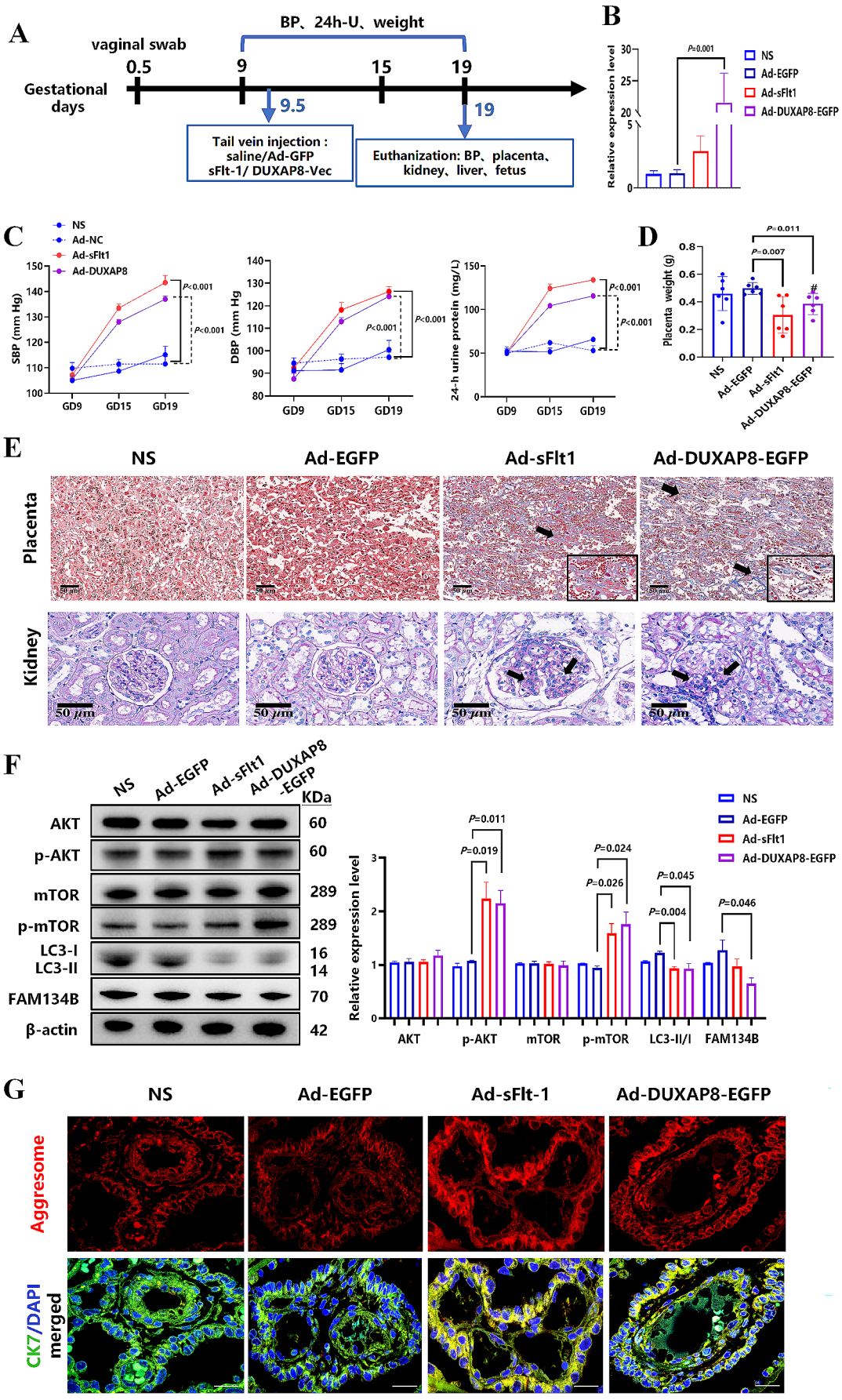
A
BP、24h-U、weight
vaginal swab
0.5
9
15
19
Gestational days
9.5
19
Tail vein injection : saline/Ad-GFP sFlt-1/ DUXAP8-Vec
Euthanization: BP、placenta、kidney、liver、fetus
B
Relative expression level
P=0.001
NS
Ad-EGFP
Ad-sFlt1
Ad-DUXAP8-EGFP
C
NS
Ad-NC
Ad-sFlt1
Ad-DUXAP8
SBP (mm Hg)
DBP (mm Hg)
24-h urine protein (mg/L)
P<0.001
GD9
GD15
GD19
D
Placenta weight (g)
P=0.011
P=0.007
E
NS
Ad-EGFP
Ad-sFlt1
Ad-DUXAP8-EGFP
Placenta
Kidney
50 μm
F
KDa
AKT
p-AKT
mTOR
p-mTOR
LC3-I
LC3-II
FAM134B
β-actin
60
289
16
14
70
42
Relative expression level
P=0.011
P=0.019
P=0.024
P=0.026
P=0.045
P=0.004
P=0.046
AKT
p-AKT
mTOR
p-mTOR
LC3-II/I
FAM134B
G
NS
Ad-EGFP
Ad-sFlt-1
Ad-DUXAP8-EGFP
Aggresome
CK7/DAPI merged

Fig. 7 DUXAP8 overexpression induces preeclampsia-like phenotypes in pregnant rats. **A** Schematic diagram of animal experimental design. **B** The expression of DUXAP8 in placenta was detected by RT-qPCR ($n=6$). **C** Systolic blood pressure (SBP) and Diastolic blood pressure (DBP) of pregnant rats were measured by tail-cuff system (GD9 and GD15) or carotid artery incubation (GD19) ($n=6$); 24-hour proteinuria levels were detected by a protein assay kit($n=6$). **D** Placental weight of pregnant rats ($n=6$). **E** Placental morphological features were identified by Masson's trichrome staining($n=6$), and the histopathologic analysis of renal tissues was detected by periodic acid Schiff ($n=6$). **F** The expression of key signaling proteins (AKT, mTOR, p-AKT^{Ser473}, p-AKT^{Thr308}, p-mTOR^{S2248}), FAM134B and LC3 proteins were detected by Western blot ($n=6$). **G** The protein aggregation in placental trophoblast cells of pregnant rats was detected by Protein Aggresome detection kit (Scale bar = 50 μm) (DAPI: nucleus; Aggresome: protein aggregates). Data are presented as mean ± SD, statistical significance was evaluated using the t-test or Mann-Whitney for 2 comparisons and two-way ANOVA for multiple comparison

Supplementary Information The online version contains supplementary material available at https://doi.org/10.1007/s00018-024-05385-y.

Author contributions X.H.W., L.Y. L. and R.Z. conceived and designed the study; X.H. W. and L.Y. L. performed experiments; X.H.W. and L.Y.L. analyzed data; L.Y.L. and Y.X.Y. performed bioinformatics analysis, and X.H.W. supervised the analysis; Q.X. and S.S.X. collected clinical tissue samples; M.L., H.Q.C. and X.H. W. verified the underlying data; X.H. W. wrote the manuscript; L.B.G. and R.Z. critically revised the manuscript. All authors have been involved in interpreting the data and approved the final version.

Funding This work was financially supported by grants from the National Key R&D Program of China (No. 2021YFC2701600; No. 2021YFC2701601), the National Natural Science Foundation of China (No. 81871175) and Sichuan Science and Technology Program (2023NSFSC1606).

Data availability The data underlying this article and further information requests for resources or reagents should be directed to and will be fulfilled by Rong Zhou (zhourong_hx@scu.edu.cn).

Declarations

Ethical approval The collection and treatment of human placenta tissues were approved by the Ethics Committee of West China Second Hospital of Sichuan University (Medical Research-2019-032), and the animal experiments were performed approved by the Ethics Committee on the Use of Animals of West China Second Hospital of Sichuan University (permit number: 2021-020).

Consent for publication All the authors have approved and agreed to publish this manuscript.

Conflict of interest None of the authors have any conflicts of interest to declare.

References

1. Rana S, Lemoine E, Granger JP, Karumanchi SA (2019) Preeclampsia: Pathophysiology, Challenges, and Perspectives Circ Res, 2019. 124(7): pp. 1094–1112.https://doi.org/10.1161/circresaha.118.313276
2. Brown MA, Magee LA, Kenny LC, Karumanchi SA, McCarthy FP, Saito S et al (2018) Hypertensive Disorders of Pregnancy: ISSHP Classification, Diagnosis, and Management Recommendations for International Practice Hypertension, 2018. 72(1): pp. 24–43.https://doi.org/10.1161/hypertensionaha.117.10803
3. Mol BWJ, Roberts CT, Thangaratinam S, Magee LA, de Groot CJM, Hofmeyr GJ (2016) Pre-eclampsia The Lancet, 2016. 387(10022): pp. 999–1011.https://doi.org/10.1016/S0140-6736(15)00070-7
4. Hitti J, Sienas L, Walker S, Benedetti TJ, Easterling T (2018) Contribution of hypertension to severe maternal morbidity Am J Obstet Gynecol, 2018. 219(4): p. 405https://doi.org/10.1016/j.ajog.2018.07.002
5. Roberts JM (2014) Pathophysiology of ischemic placental disease Semin Perinatol, 2014. 38(3): pp. 139–45https://doi.org/10.1053/j.semperi.2014.03.005
6. Aplin JD, Myers JE, Timms K, Westwood M (2020) Tracking placental development in health and disease Nat Rev Endocrinol, 2020. 16(9): pp. 479–494.https://doi.org/10.1038/s41574-020-0372-6
7. Yu X, Wu H, Yang Y, Wang F, Wang Y-L, Shao X (2022) Placental Development and Pregnancy-Associated Diseases Maternal-Fetal Medicine, 2022. 4(1): pp. 36–51.https://doi.org/10.1097/fm9.0000000000000134
8. Buhimschi IA, Nayeri UA, Zhao G, Shook LL, Pensalfini A, Funai EF et al (2014) Protein misfolding, congophilia, oligomerization, and defective amyloid processing in preeclampsia Sci Transl Med, 2014. 6(245): p. 245https://doi.org/10.1126/scitranslmed.3008808
9. Cheng SB, Nakashima A, Sharma S (2016) Understanding Pre-Eclampsia Using Alzheimer's Etiology: An Intriguing Viewpoint Am J Reprod Immunol, 2016. 75(3): pp. 372–81.https://doi.org/10.1111/aji.12446
10. Gerasimova EM, Fedotov SA, Kachkin DV, Vashukova ES, Glotov AS, Chernoff YO, Rubel AA (2019) Protein Misfolding during Pregnancy: New Approaches to Preeclampsia Diagnostics Int J Mol Sci, 2019. 20(24)https://doi.org/10.3390/ijms20246183
11. McCarthy FP, Adetoba A, Gill C, Bramham K, Bertolaccini M, Burton GJ et al (2016) Urinary congophilia in women with hypertensive disorders of pregnancy and preexisting proteinuria or hypertension Am J Obstet Gynecol, 2016. 215(4): p. 464https://doi.org/10.1016/j.ajog.2016.04.041
12. Kalkunte SS, Neubeck S, Norris WE, Cheng SB, Kostadinov S, Vu D, Hoang et al (2013) Transthyretin is dysregulated in preeclampsia, and its native form prevents the onset of disease in a preclinical mouse model Am J Pathol, 2013. 183(5): pp. 1425–1436.https://doi.org/10.1016/j.ajpath.2013.07.022
13. Tong M, Cheng SB, Chen Q, DeSousa J, Stone PR, James JL et al (2017) Aggregated transthyretin is specifically packaged into

placental nano-vesicles in preeclampsia Sci Rep, 2017. 7(1): p. 6694https://doi.org/10.1038/s41598-017-07017-x
14. Klionsky DJ, Petroni G, Amaravadi RK, Baehrecke EH, Ballabio A, Boya P et al (2021) Autophagy in major human diseases Embo j, 2021. 40(19): p. ehttps://doi.org/10.15252/embj.2021108863
15. Nakashima A, Cheng SB, Ikawa M, Yoshimori T, Huber WJ, Menon R et al (2020) Evidence for lysosomal biogenesis proteome defect and impaired autophagy in preeclampsia Autophagy, 2020. 16(10): pp. 1771–1785.https://doi.org/10.1080/15548627.2019.1707494
16. Nakashima A, Shima T, Tsuda S, Aoki A, Kawaguchi M, Furuta A et al (2021) Aggrephagy Deficiency in the Placenta: A New Pathogenesis of Preeclampsia Int J Mol Sci, 2021. 22(5).https://doi.org/10.3390/ijms22052432
17. Nakashima A, Tsuda S, Kusabiraki T, Aoki A, Ushijima A, Shima T et al (2019) Current Understanding of Autophagy in Pregnancy Int J Mol Sci, 2019. 20(9).https://doi.org/10.3390/ijms20092342
18. Nakashima A, Yamanaka-Tatematsu M, Fujita N, Koizumi K, Shima T, Yoshida T et al (2013) Impaired autophagy by soluble endoglin, under physiological hypoxia in early pregnant period, is involved in poor placentation in preeclampsia Autophagy, 2013. 9(3): pp. 303–16.https://doi.org/10.4161/auto.22927
19. Nakashima A, Shima T, Aoki A, Kawaguchi M, Yasuda I, Tsuda S et al (2020) Placental autophagy failure: a risk factor for preeclampsia. J Obstet Gynaecol Res 2020. https://doi.org/10.1111/jog.14489
20. Li W, He P, Huang Y, Li YF, Lu J, Li M et al (2021) Selective autophagy of intracellular organelles: recent research advances Theranostics, 2021. 11(1): pp. 222–256.https://doi.org/10.7150/thno.49860
21. Borgese N, Francolini M, Snapp E (2006) Endoplasmic reticulum architecture: structures in flux Curr Opin Cell Biol, 2006. 18(4): pp. 358–64.https://doi.org/10.1016/j.ceb.2006.06.008
22. Mochida K, Oikawa Y, Kimura Y, Kirisako H, Hirano H, Ohsumi Y, Nakatogawa H (2015) Receptor-mediated selective autophagy degrades the endoplasmic reticulum and the nucleus Nature, 2015. 522(7556): pp. 359–62https://doi.org/10.1038/nature14506
23. Okamoto K (2014) Organellophagy: eliminating cellular building blocks via selective autophagy J Cell Biol, 2014. 205(4): pp. 435–45.https://doi.org/10.1083/jcb.201402054
24. Khaminets A, Heinrich T, Mari M, Grumati P, Huebner AK, Akutsu M et al (2015) Regulation of endoplasmic reticulum turnover by selective autophagy Nature, 2015. 522(7556): pp. 354-8https://doi.org/10.1038/nature14498
25. Mallucci GR, Klenerman D, Rubinsztein DC (2020) Developing Therapies for Neurodegenerative Disorders: Insights from Protein Aggregation and Cellular Stress Responses Annu Rev Cell Dev Biol, 2020. 36: pp. 165–189.https://doi.org/10.1146/annurev-cellbio-040320-120625
26. Schultz ML, Krus KL, Lieberman AP (2016) Lysosome and endoplasmic reticulum quality control pathways in Niemann-Pick type C disease Brain Res, 2016. 1649(Pt B): pp. 181–188.https://doi.org/10.1016/j.brainres.2016.03.035
27. Oo JA, Brandes RP, Leisegang MS (2022) Long non-coding RNAs: novel regulators of cellular physiology and function Pflugers Arch, 2022. 474(2): pp. 191–204.https://doi.org/10.1007/s00424-021-02641-z
28. Sun M, Nie FQ, Zang C, Wang Y, Hou J, Wei C et al (2017) The Pseudogene DUXAP8 Promotes Non-small-cell Lung Cancer Cell Proliferation and Invasion by Epigenetically Silencing EGR1 and RHOB Mol Ther, 2017. 25(3): pp. 739–751.https://doi.org/10.1016/j.ymthe.2016.12.018
29. Lin MG, Hong YK, Zhang Y, Lin BB, He XJ (2018) Mechanism of lncRNA DUXAP8 in promoting proliferation of bladder cancer cells by regulating PTEN Eur Rev Med Pharmacol Sci, 2018. 22(11): pp. 3370–3377.https://doi.org/10.26355/eurrev_201806_15158
30. Li LM, Hao SJ, Ni M, Jin S, Tian YQ (2021) DUXAP8 promotes the proliferation and migration of ovarian cancer cells via down-regulating microRNA-29a-3p expression Eur Rev Med Pharmacol Sci, 2021. 25(4): pp. 1837–1844.https://doi.org/10.26355/eurrev_202102_25078
31. Wang B, Xu W, Cai Y, Chen J, Guo C, Zhou G, Yuan C (2022) DUXAP8: A Promising lncRNA with Carcinogenic Potential in Cancer Curr Med Chem, 2022. 29(10): pp. 1677–1686.https://doi.org/10.2174/0929867328666210726092020
32. Soares MJ, Chakraborty D, Karim Rumi MA, Konno T, Renaud SJ (2012) Rat placentation: an experimental model for investigating the hemochorial maternal-fetal interface Placenta, 2012. 33(4): pp. 233–43.https://doi.org/10.1016/j.placenta.2011.11.026
33. Yoon JH, Abdelmohsen K, Gorospe M (2013) Posttranscriptional gene regulation by long noncoding RNA J Mol Biol, 2013. 425(19): pp. 3723-30.https://doi.org/10.1016/j.jmb.2012.11.024
34. You F, Sun H, Zhou X, Sun W, Liang S, Zhai Z, Jiang Z (2009) PCBP2 mediates degradation of the adaptor MAVS via the HECT ubiquitin ligase AIP4 Nat Immunol, 2009. 10(12): pp. 1300-8https://doi.org/10.1038/ni.1815
35. Verhoef LG, Heinen C, Selivanova A, Halff EF, Salomons FA, Dantuma NP (2009) Minimal length requirement for proteasomal degradation of ubiquitin-dependent substrates FASEB J, 2009. 23(1): pp. 123–33.https://doi.org/10.1096/fj.08-115055
36. Zeisler H, Llurba E, Chantraine F, Vatish M, Staff AC, SennstrÃ¶m M et al (2016) Predictive Value of the sFlt-1:PlGF Ratio in Women with Suspected Preeclampsia N Engl J Med, 2016. 374(1): pp. 13–22.https://doi.org/10.1056/NEJMoa1414838
37. Stepan H, Galindo A, Hund M, Schlembach D, Sillman J, Surbek D, Vatish M (2023) Clinical utility of sFlt-1 and PlGF in screening, prediction, diagnosis and monitoring of pre-eclampsia and fetal growth restriction Ultrasound Obstet Gynecol, 2023. 61(2): pp. 168–180.https://doi.org/10.1002/uog.26032
38. Lei C, Li S, Fan Y, Hua L, Pan Q, Li Y et al (2022) LncRNA DUXAP8 induces breast cancer radioresistance by modulating the PI3K/AKT/mTOR pathway and the EZH2-E-cadherin/RHOB pathway Cancer Biol Ther, 2022. 23(1): pp. 1–13.https://doi.org/10.1080/15384047.2022.2132008
39. Ji X, Tao R, Sun LY, Xu XL and W. Ling(down-regulation of long non-coding RNA DUXAP8 suppresses proliferation, metastasis and EMT by modulating miR-498 through TRIM44-mediated AKT/mTOR pathway in non-small-cell lung cancer
40. Tang X, Cao Y, Wu D, Sun L, Xu Y (2023) Downregulated DUXAP8 lncRNA impedes trophoblast cell proliferation and migration by epigenetically upregulating TFPI2 expression Reprod Biol Endocrinol, 2023. 21(1): p. 58https://doi.org/10.1186/s12958-023-01108-3
41. Yuan C, Chen M, Cai X (2021) Advances in poly(rC)-binding protein 2: Structure, molecular function, and roles in cancer Biomed Pharmacother, 2021. 139: p. 111719https://doi.org/10.1016/j.biopha.2021.111719
42. Makeyev AV, Liebhaber SA (2002) The poly(C)-binding proteins: a multiplicity of functions and a search for mechanisms Rna, 2002. 8(3): pp. 265–78.https://doi.org/10.1017/s1355838202024627
43. Georgiadou D, Boussata S, Keijser R, Janssen DAM, Afink GB, van Dijk M (2021) Knockdown of Splicing Complex Protein PCBP2 Reduces Extravillous Trophoblast Differentiation Through Transcript Switching Front Cell Dev Biol, 2021. 9: p. 671806https://doi.org/10.3389/fcell.2021.671806
44. Guo S, Chen Y, Yang Y, Zhang X, Ma L, Xue X et al (2021) TRIB2 modulates proteasome function to reduce ubiquitin stability and protect liver cancer cells against oxidative stress Cell Death Dis, 2021. 12(1): p. 42.https://doi.org/10.1038/s41419-020-03299-8

45. Weel IC, Ribeiro VR, Romão-Veiga M, Fioratti EG, Peraçoli JC (2023) and M.T.S. Peraçoli Down-regulation of autophagy proteins is associated with higher mTOR expression in the placenta of pregnant women with preeclampsia Braz J Med Biol Res, 2023. 55: p. e12283https://doi.org/10.1590/1414-431X2022e12283
46. Oh SY, Choi SJ, Kim KH, Cho EY, Kim JH, Roh CR (2008) Autophagy-related proteins, LC3 and Beclin-1, in placentas from pregnancies complicated by preeclampsia Reprod Sci, 2008. 15(9): pp. 912–20.https://doi.org/10.1177/1933719108319159
47. Curtis S, Jones CJ, Garrod A, Hulme CH, Heazell AE (2013) Identification of autophagic vacuoles and regulators of autophagy in villous trophoblast from normal term pregnancies and in fetal growth restriction J Matern Fetal Neonatal Med, 2013. 26(4): pp. 339–46https://doi.org/10.3109/14767058.2012.733764
48. Hung TH, Hsieh TT, Chen SF, Li MJ, Yeh YL (2013) Autophagy in the human placenta throughout gestation PLoS One, 2013. 8(12): p. ehttps://doi.org/10.1371/journal.pone.0083475
49. Akaishi R, Yamada T, Nakabayashi K, Nishihara H, Furuta I, Kojima T et al (2014) Autophagy in the placenta of women with hypertensive disorders in pregnancy Placenta, 2014. 35(12): pp. 974–80.https://doi.org/10.1016/j.placenta.2014.10.009
50. Kim YC, Guan KL (2015) mTOR: a pharmacologic target for autophagy regulation J Clin Invest, 2015. 125(1): pp. 25–32.https://doi.org/10.1172/JCI73939
51. Settembre C, Zoncu R, Medina DL, Vetrini F, Erdin S, Erdin S et al (2012) A lysosome-to-nucleus signalling mechanism senses and regulates the lysosome via mTOR and TFEB Embo j, 2012. 31(5): pp. 1095–108.https://doi.org/10.1038/emboj.2012.32
52. Yuan HX, Russell RC, Guan KL (2013) Regulation of PIK3C3/VPS34 complexes by MTOR in nutrient stress-induced autophagy Autophagy, 2013. 9(12): pp. 1983-95.https://doi.org/10.4161/auto.26058
53. Weel IC, Ribeiro VR, RomÃ£o-Veiga M, Fioratti EG, PeraÃ§oli JC (2023) and M.T.S. PeraÃ§oli Down-regulation of autophagy proteins is associated with higher mTOR expression in the placenta of pregnant women with preeclampsia Braz J Med Biol Res, 2023. 55: p. e12283https://doi.org/10.1590/1414-431X2022e12283
54. Cheng S, Huang Z, Banerjee S, Jash S, Buxbaum JN, Sharma S (2022) Evidence From Human Placenta, Endoplasmic Reticulum-Stressed Trophoblasts, and Transgenic Mice Links Transthyretin Proteinopathy to Preeclampsia Hypertension, 2022. 79(8): pp. 1738–1754.https://doi.org/10.1161/hypertensionaha.121.18916
55. Oikonomou C, Hendershot LM (2020) Disposing of misfolded ER proteins: A troubled substrate's way out of the ER Mol Cell Endocrinol, 2020. 500: p. 110630https://doi.org/10.1016/j.mce.2019.110630
56. Stolz A, Grumati P (2019) The various shades of ER-phagy Febs j, 2019. 286(23): pp. 4642–4649.https://doi.org/10.1111/febs.15031
57. Napolitano G, Di Malta C, Esposito A, de Araujo MEG, Pece S, Bertalot G et al (2020) A substrate-specific mTORC1 pathway underlies Birt-Hogg-DubÃ© syndrome Nature, 2020. 585(7826): pp. 597–602.https://doi.org/10.1038/s41586-020-2444-0
58. Martina JA, Chen Y, Gucek M, Puertollano R (2012) MTORC1 functions as a transcriptional regulator of autophagy by preventing nuclear transport of TFEB Autophagy, 2012. 8(6): pp. 903–14.https://doi.org/10.4161/auto.19653
59. Fraiberg M, Elazar Z (2020) Selective autophagy bears bone Embo j, 2020. 39(17): p. ehttps://doi.org/10.15252/embj.2020105965
60. He L, Qian X, Cui Y (2021) Advances in ER-Phagy and Its Diseases Relevance Cells, 2021. 10(9)https://doi.org/10.3390/cells10092328
61. Hill MA, Sykes AM, Mellick GD (2023) ER-phagy in neurodegeneration J Neurosci Res, 2023. 101(10): pp. 1611–1623.https://doi.org/10.1002/jnr.25225
62. Kasem K, Sullivan E, Gopalan V, Salajegheh A, Smith RA, Lam AK (2014) JK1 (FAM134B) represses cell migration in colon cancer: a functional study of a novel gene Exp Mol Pathol, 2014. 97(1): pp. 99–104.https://doi.org/10.1016/j.yexmp.2014.06.002
63. Tang WK, Chui CH, Fatima S, Kok SH, Pak KC, Ou TM et al (2007) Oncogenic properties of a novel gene JK-1 located in chromosome 5p and its overexpression in human esophageal squamous cell carcinoma Int J Mol Med, 2007. 19(6): pp. 915–23
64. Murphy SR, LaMarca BB, Cockrell K, Granger JP (2010) Role of endothelin in mediating soluble fms-like tyrosine kinase 1-induced hypertension in pregnant rats Hypertension, 2010. 55(2): pp. 394-8https://doi.org/10.1161/hypertensionaha.109.141473